Section (A)

Characterization of PMMA/perylene

(IV.A.1) Differential Scanning calorimetery (DSC)

Fig. (IV.1) shows the DSC thermograms for pure PMMA samples recorded at heating rate of 20 °C/min, as a representative diagram for all investigated PMMA/perylene samples. The characteristic features are: first, the glass transition temperature T_g for thermally prepared samples is higher than that of solvent cast samples. Second, an endothermic peak appears at a temperature T_s for solvent cast samples, which refers to the evaporation of solvent, in agreement with published data [37]. After a second scan of these samples above T_g the endothermic peak disappeared (The DSC curves became similar to that for thermally prepared samples). These results showed that the solvent molecules are retained in all casting samples inducing a decrease in T_g [116]. The values of T_g and T_s are listed in Table (IV.1).

The change in T_g by increasing the dye concentration can be understood by the following effects:

(i) The large size of dye molecules may fill the free volume, this leads to decrease the free volume and the chain flexibility (increasing T_g).

(ii) The number of end groups may increase, this leads to the increase in free volume and consequently the chain flexibility (lowering in T_g).

In general for lower dye contents in thermally prepared samples and all solvent cast samples the first effect is more pronounced.

The apparent increase in T_s by increasing dye contents refers to

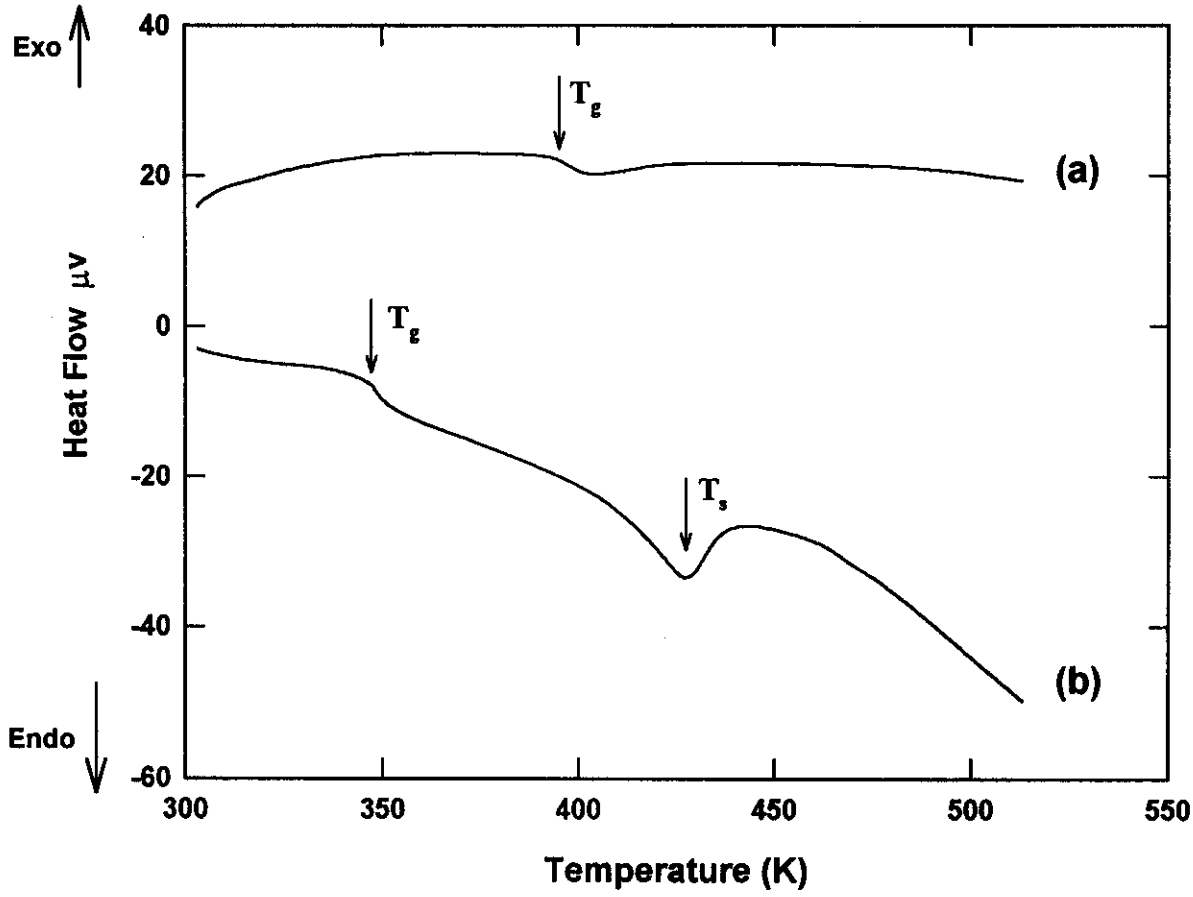

Fig.(IV.1) **DSC thermograms of (a) thermally polymerized and (b) solvent-cast PMMA samples.**

Table (IV.1): The values of T_g and T_s for (PMMA/perylene) samples.

Dye concentration mol. %	T_g (K)	T_s (K)
Thermally polymerized		
0.00	395.4	.....
5.28×10^{-5}	395.8	.....
6.33×10^{-5}	399.0	.....
7.92×10^{-5}	401.5	.....
1.06×10^{-4}	394.6	.....
1.37×10^{-4}	391.9	.....
2.11×10^{-4}	391.3	.....
Solvent cast		
0.0	346.5	415.7
1.78×10^{-4}	347.2	426.8
5.00×10^{-4}	348.4	435.3

the aggregation of dye molecules compared to that of the side group of the polymer, which tends to hinder the total evaporation of solvent and trap it between chains [86].

(IV.A.2) FT-IR Measurements

FT-IR spectra of PMMA and PMMA/perylene prepared by solvent casting and thermal polymerization were studied. Table (IV.2) summarizes the obtained wavenumber of the characteristic peaks. It is noticed that the samples prepared by thermal procedure are completely polymerized due to the disappearance of aliphatic C=C characterizing MMA [116]. Furthermore the wave number of the main chain groups of thermally polymerized samples appears at shorter wavenumber in comparison to that in solvent cast one. This means that the thermally polymerized samples are more stable than the solvent cast, because the vibrational energies of the main chain bonds (phonon energies) are lower. Moreover in the solvent cast samples the solvent is not completely evaporated due to the appearance of C-CL peak characterizing chloroform [116,118].

The effect of perylene concentration is observed in Table (IV.2), the wave number of the C=O group shifts gradually to higher values by increasing dye concentration. At higher perylene concentrations for thermally polymerized samples (higher than 7.92×10^{-5}mol.%), the wave -number of C=O peak decreases due to the aggregation of dye molecules.

In addition the peak position of aromatic C = C group of perylene (1600-1475 cm^{-1}) is not affected by the sample preparation. This means

ıble (IV.2): The wavenumber (cm^{-1}) of the characteristic groups in PMMA/perylene samples.

(a) Thermally polymerized

Concentration mol.%	-C-CH_3	-C-CH_2-C-	C = O (ester)	C - O (ester)	C - H (aromatic)	C = C (aromatic)
0.00	1735.0	1445.3	1734.3	1117.2	-----	-----
5.28×10^{-5}	1460.5	1451.1	1737.2	1107. 8	3082.6	1647.7 1508.8
6.33×10^{-5}	1371.1	1481.0	1742.1	1107.5 1229.2	3076.3	1639.2
7.92×10^{-5}	1459.6	1454.9	1745.8	1257.8	3022.0	1648.4 1508.5
1.06×10^{-4}	1463.7	1431.0	1736.5	1105.2	3082.3	1647.6
1.37×10^{-4}	1461.1	1449.0	1734.0	1226.5	3026.8	1508.6
2.11×10^{-4}	1370.6	1445.7	1731.1	1112.5 1234.7	3022.8	1646.8 1508.4

(b) Solvent cast

centration nol.%	-C-CH_3	-C-CH_2-C-	C = O (ester)	C - O (ester)	C - H (aromatic)	C = C (aromatic)	C-Cl
0.00	2953.1	2843.7	1734.4	1069.2 1080.8	-----	-----	656.2
'8 x 10^{-4}	2968.7	2937.5 2845.9	1738.2	1098.7	3090.2	1508.6 1575.0	664.9
)0 x 10^{-4}	2960.9	2926.1 2852.9	1742.2	1070.3	3082.3	1508.9 1647.7	724.8

property show that PMMA is a good matrix for laser dyes and acts as inert medium.

FT-IR measurements were also carried out to detect the influence long-term exposure to the intense direct light from Xenon arc lamp on thermally polymerized PMMA/Perylene sample of concentration (6.33 x 10^{-5} mol.%). Fig.(IV.2) shows that FT-IR spectrum of the sample after irradiation for 24 hours changed strongly, due to the severe degradation of both the polymer and dye. This can be interpreted as follows, the short wave UV radiation have sufficient energy to enhance bond dissociation of C=O peak (characterizing PMMA) and aromatic C-H peak (characterizing perylene)[116,137]. So it is important to filter out the short wave UV part of the sunlight completely (i.e. good UV protective), especially for space solar applications (such as spacecraft power and satellite communications), where the space is rich of UV radiation[138].

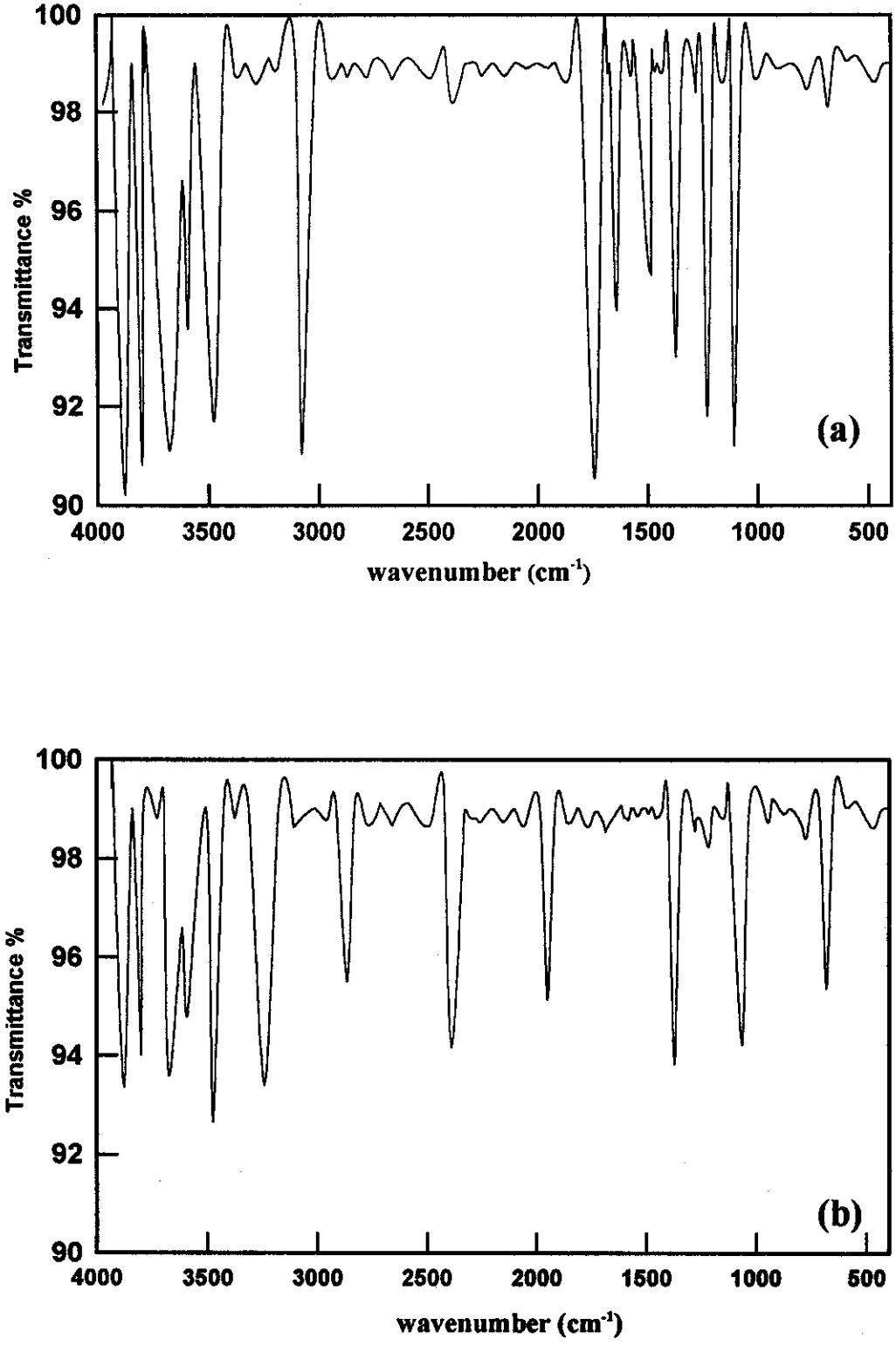

Fig.(IV.2) FT-IR spectra of thermally polymerized PMMA /Perylene sample (a)Before and (b)after irradiation for 24 hours with unfiltered light.

Section (B)

Electrical Conductivity of PMMA/perylene

(IV.B.1) DC Conductivity

The electrical conductivity of pure PMMA samples and those doped by different concentrations of perylene dye have been studied in the temperature range (303-433K). Fig.(IV.3) represents the semi-logarithmic plots of σ vs $10^3/T$ for all the samples investigated. It is noticed that the electrical conductivity is thermally activated up to a peak value σ_p at a certain temperature T_p lies in the same range of the glass transition temperature determined by DSC measurements. The activated part in σ-$10^3/T$ relation can be attributed to the fact that PMMA is described as a basic polymer or an electron donor. According to the Lewis concept [139,140], the presence of ester functional groups, with the carbonyl oxygen atom being a basic site, is the reason why PMMA exhibits electron donor ability. So the conduction process occurs by the electron jumping (hopping or tunneling) between filled and empty sites located in the energy band gap. The conduction mechanism would be confirmed in the present study by using ac conductivity measurements. This activated part could be described according to the following Arrhenius relation [136],

$$\sigma = \sigma_o \exp(-\Delta E/k_B T) \qquad \text{(IV-1)}$$

where σ_o is the temperature independent parameter , ΔE is the activation energy of conduction and k is Boltzmann's constant. The values of ΔE, σ_o, σ_p and T_p are obtained and listed in Table (IV.3).

On the other hand, the attenuated part in the conduction process

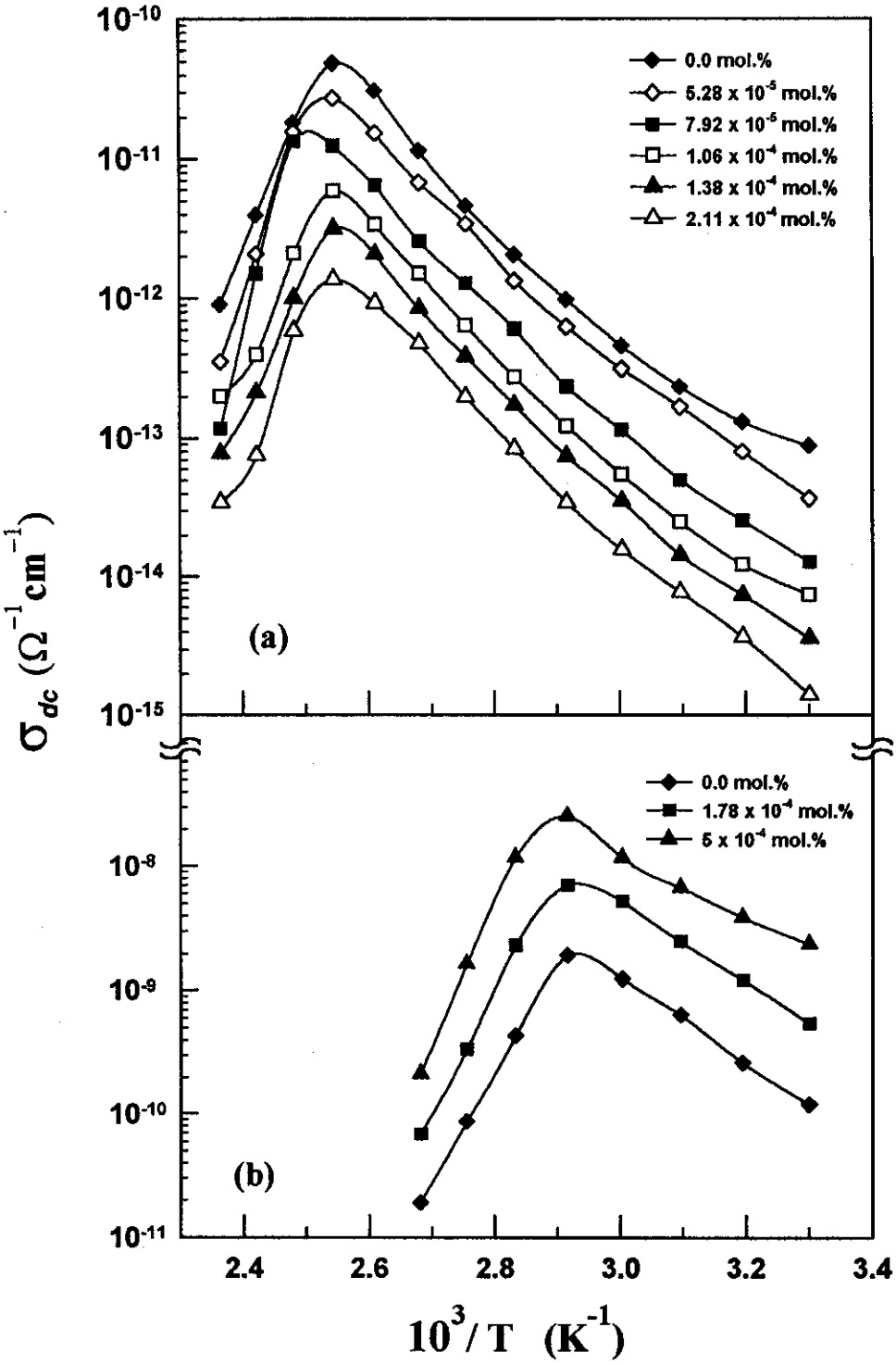

Fig.(IV.3) Temperature dependence of dc electrical conductivity, σ_{dc}, for PMMA and PMMA/Perylene samples prepared by ,(a) thermal polymerization and (b)solvent casting methods.

Table (IV. 3): The calculated values of ΔE_{dc}, σ_p, T_p and σ_o for (PMMA/perylene) samples.

concentration mol. %	ΔE (eV)	$\sigma_p(\Omega^{-1}.cm^{-1})$	$T_P(K)$	σ_o ($\Omega^{-1}.cm^{-1}$)
Thermally polymerized				
0.00	0.755	$6.76x10^{-11}$	395	0.239
$6.33x10^{-5}$	0.761	$2.75x10^{-11}$	396	0.131
$7.92x10^{-5}$	0.786	$1.35x10^{-11}$	402	0.112
$1.06x10^{-4}$	0.795	$5.93x10^{-12}$	394	0.078
$1.37x10^{-4}$	0.801	$3.19x10^{-12}$	392	0.055
$2.11x10^{-4}$	0.808	$1.38x10^{-12}$	391	0.033
Solvent cast				
0.00	0.641	$1.95x10^{-9}$	341	5.830
$1.78x10^{-4}$	0.590	$7.08x10^{-9}$	343	3.830
$5.00x10^{-4}$	0.520	$2.56x10^{-8}$	347	1.010

On the other hand, the attenuated part in the conduction process above T_p could be explained by the fact that the conduction process is opposed by the large deformations characteristic of the viscoelastic state permitted by segmental motions [141]. In other words beyond T_g the electron phonon coupling becomes more pronounced which results in the charge carrier scattering and consequently a reduction of the charge carrier mobility.

The effect of the sample preparation on the dc conductivity is shown in Fig.(IV.3). The conductivity values obtained for solvent cast samples found to be higher by two orders of magnitude than the thermally prepared samples. This can be explained as follows, PMMA and chloroform may form acid base complexes resulting from the interactions between the ester basic group of PMMA and hydrogen acid atom of chloroform [139,140]. So the confined chloroform molecules in the main chain surrounding of polymer will lead to an increase of the density of localized states which enhances the probability of electron jumping.

Fig.(IV.4) shows the dye concentration dependence of dc conductivity. The incorporation of perylene dye to PMMA results in a remarkable change of dc conductivity obeying the following empirical equation,

$$\sigma = \sigma^* e^{\pm c/c_o} \qquad \textbf{(IV-2)}$$

where σ^* is a concentration independent parameter equals σ at $\mathbf{c} = 0$ and $\mathbf{c_o}$ is the characteristic concentration. The positive or negative sign of the exponent in equation (IV-2) mentioned to rise or reduction of the conductivity with perylene concentration (it depends on the preparation

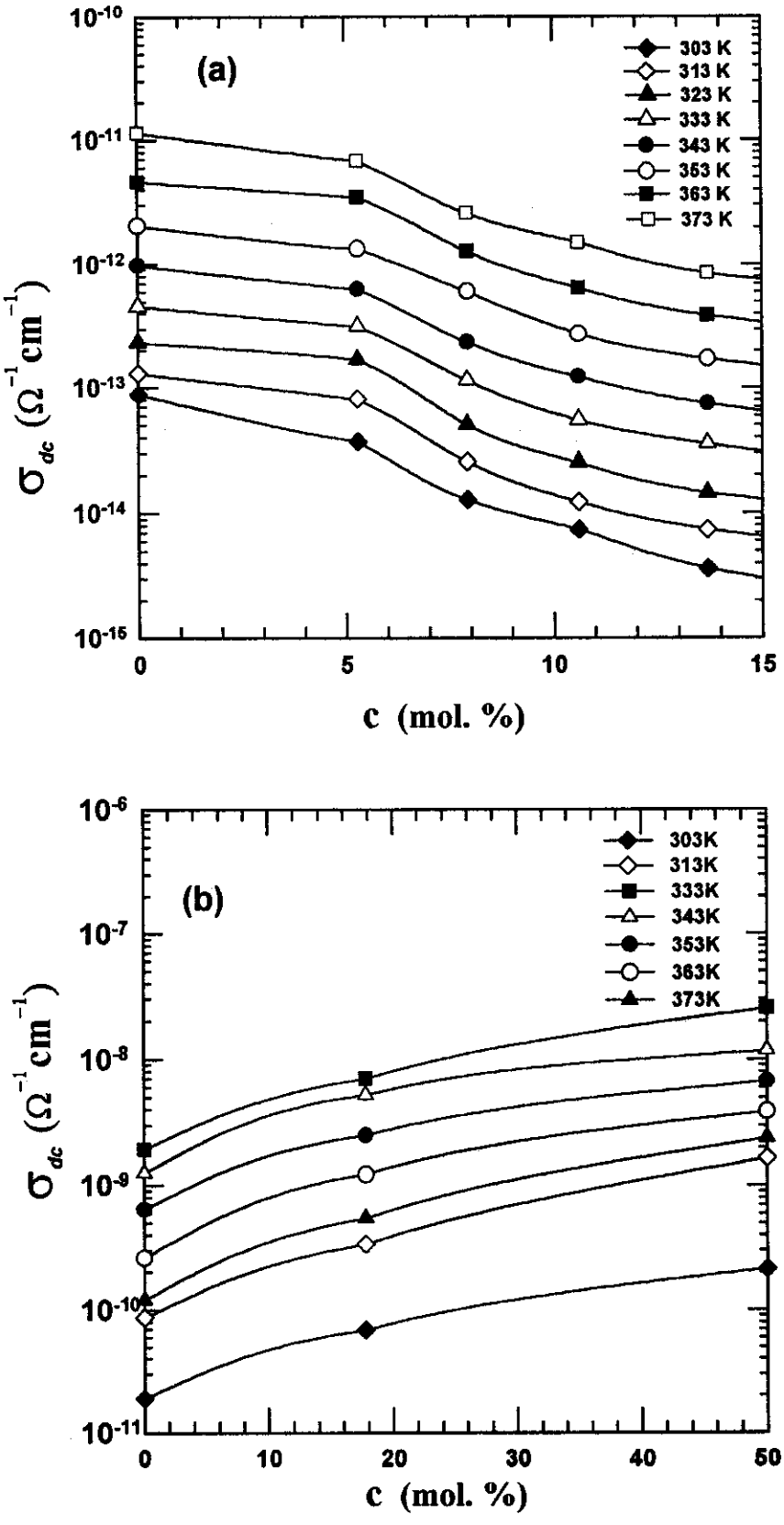

Fig.(IV.4) Concentration dependence of dc electrical conductivity , σ_{dc}, for PMMA/Perylene samples, (a) thermally polymerized and (b)solvent cast.

method). In the case of thermally prepared samples, σ attenuates by increasing dye contents. This can be explained by the following: the increase of perylene dye results in an increase in the scattering of charge carriers, since the attachment of large size dye molecules hinder the conduction process. In the case of solvent cast samples σ increases by increasing the concentration of the dye. This can be explained by the fact that the dye aggregates results in a confusion of solvent molecules which acts as a carrier acceptor in the polymer matrix (this has been confirmed by DSC measurements). The values of $\mathbf{c}_o$ and σ* are estimated at different temperatures for all the investigated samples and listed in Table (IV.4).It is shown that $\mathbf{c}_o$ increases by increasing the temperature up to T_p (near T_g) and then attenuates to lower values.

(IV.B.2) AC Conductivity

The frequency dependence of the total conductivity $\sigma_{tot.}(\omega)$ of (PMMA/Perylene) samples was studied in the temperature range (303-433K) and frequency range (10^3- $5x10^6$ Hz) . Fig. (IV.5) illustrates the frequency dependence of $\sigma_{tot.}(\omega)$ for pure PMMA samples at different temperatures, which represents a typical plot for all investigated samples. It is evident that the frequency independent conductivity appears at low frequency range, whereas the frequency dependent conductivity appears at moderate frequency ranges. Therefore, the frequency dependence of the total conductivity could be given by the following relation [142-144],

$$\sigma_{tot}(\omega) = \sigma_{dc} + \sigma_{ac} = \sigma_{dc} + A\omega^s \qquad \textbf{(IV-3)}$$

where σ_{dc} is a frequency independent term representing the dc component and A is the frequency independent factor. The values of the

Table (IV.4): The values of the characteristic concentration , c_o (mol.%), at different temperatures for PMMA/perylene samples .

T (K)	Thermally Polymerized	Solvent cast
303	$4.78x10^{-5}$	$2.70x10^{-5}$
313	$5.43x10^{-5}$	$3.06x10^{-5}$
323	$5.60x10^{-5}$	$3.50x10^{-5}$
333	$5.16x10^{-5}$	$3.70x10^{-5}$
343	$5.84x10^{-5}$	$3.15x10^{-5}$
353	$6.08x10^{-5}$	$2.50x10^{-5}$
363	$6.07x10^{-5}$	$2.70x10^{-5}$
373	$6.15x10^{-5}$	$3.37x10^{-5}$
383	$5.71x10^{-5}$	$3.85x10^{-5}$
393	$5.50x10^{-5}$	$4.60x10^{-5}$
403	$5.17x10^{-5}$	.....
413	$4.91x10^{-5}$	.....
423	$6.58x10^{-5}$	.....

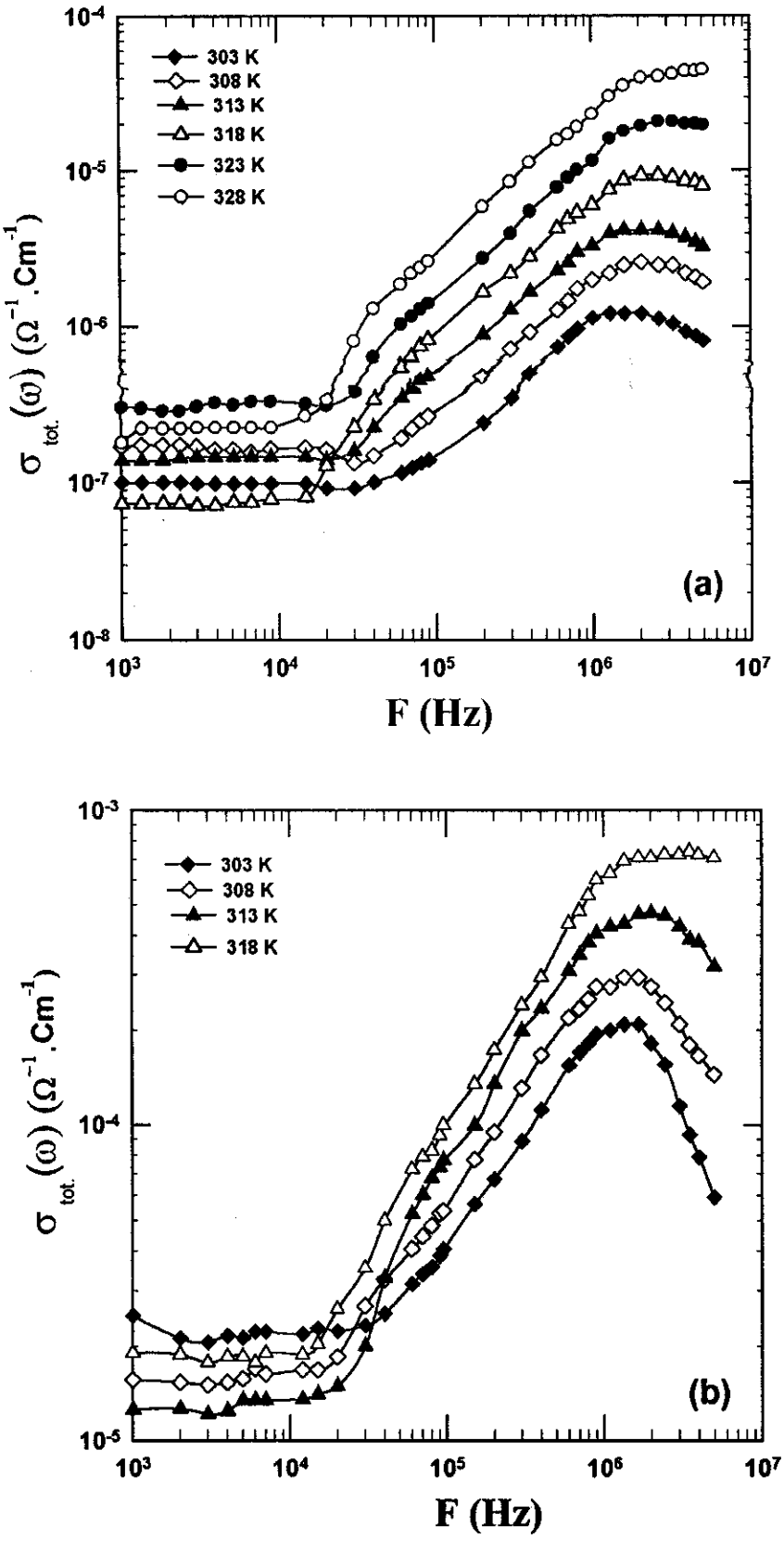

Fig.(IV.5) Frequency dependence of the total conductivity, σ_{tot}, for pure PMMA prepared by, (a) thermal polymerization and (b)solvent casting methods.

exponent s are deduced at different temperatures for all the samples investigated using the least square fitting of equation (IV-3) and are summarized in Table (IV.5). Fig. (IV.6) shows the temperature dependence of exponent s, it is noted that a peak is observed in s-T relation for both thermally prepared and solvent cast samples. The peak temperature is significantly correlated to T_g of the samples. In addition, the observed increase of s by increasing temperature up to the peak can be explained according to the quantum mechanical tunneling model (QMT)[102-105] and is given by the following relation [100]

$$s = 1-\{4 / |\ln (1 / \omega\tau_o) - W_H / k_BT|\} \qquad \text{(IV-4)}$$

where ω is the angular frequency and τ_o is the relaxation time, k_B is Boltzmann's constant and W_H is the activation energy of a single electron transport between degenerate sites. ($W_H \cong W_P/2$) where W_p is the polaron hopping energy. It should also be noted that a temperature dependent frequency exponent can arise from (QMT) model when the carrier motion occurs within clusters. On the other hand the observed decrease of s values beyond the peak by increasing temperature can be understood on the basis of the change in conduction mechanism which is based on correlated barrier hopping (CBH) model [145]. The exponent s increases towards unity as T tends to the absolute zero according to the relation [102]:

$$s = 1-\{6\ k_BT/W_M\} \qquad \text{(IV-5)}$$

where W_M is the effective barrier for single electron hopping. This confirms the dc conduction mechanism.

The temperature dependence of $\sigma_{tot.}(\omega)$ for the pure PMMA

Table (IV.5): The obtained values of the exponent (s) at different temperatures for PMMA/perylene samples.

Concentration (mol. %)	303 K	313 K	323 K	333 K	343 K	353 K	363 K	373 K	383 K	393 K	403 K	413 K	423 K
Thermally polymerized													
0.00	0.811	0.832	0.837	0.892	0.925	0.908	1.011	1.066	1.014	0.922	0.789	0.697	0.688
6.33×10^{-5}	0.640	0.752	0.755	0.854	0.798	0.897	0.977	1.025	1.045	1.011	0.940	0.816	0.727
7.92×10^{-5}	0.610	0.748	0.759	0.791	0.839	0.885	0.966	1.007	1.042	1.047	0.973	0.818	0.762
1.06×10^{-4}	0.580	0.729	0.727	0.776	0.815	0.863	0.920	1.021	1.028	1.032	0.943	0.841	0.827
1.38×10^{-4}	0.550	0.666	0.707	0.760	0.771	0.843	0.953	0.990	1.017	0.996	0.900	0.777	0.690
2.11×10^{-4}	0.616	0.718	0.852	0.947	0.995	0.963	0.930	0.774	0.729	0.721	0.681	0.642	0.520
Solvent cast													
0.00	0.628	0.108	0.844	0.807	0.946	0.940	0.842	0.770	0.682	0.680	------	------	------
1.78×10^{-5}	0.726	0.743	0.785	0.787	0.962	0.978	0.875	0.814	0.730	0.721	------	------	------
5.00×10^{-4}	0.737	0.771	0.784	0.829	0.875	1.005	0.974	0.890	0.850	0.847	-----	-----	-----

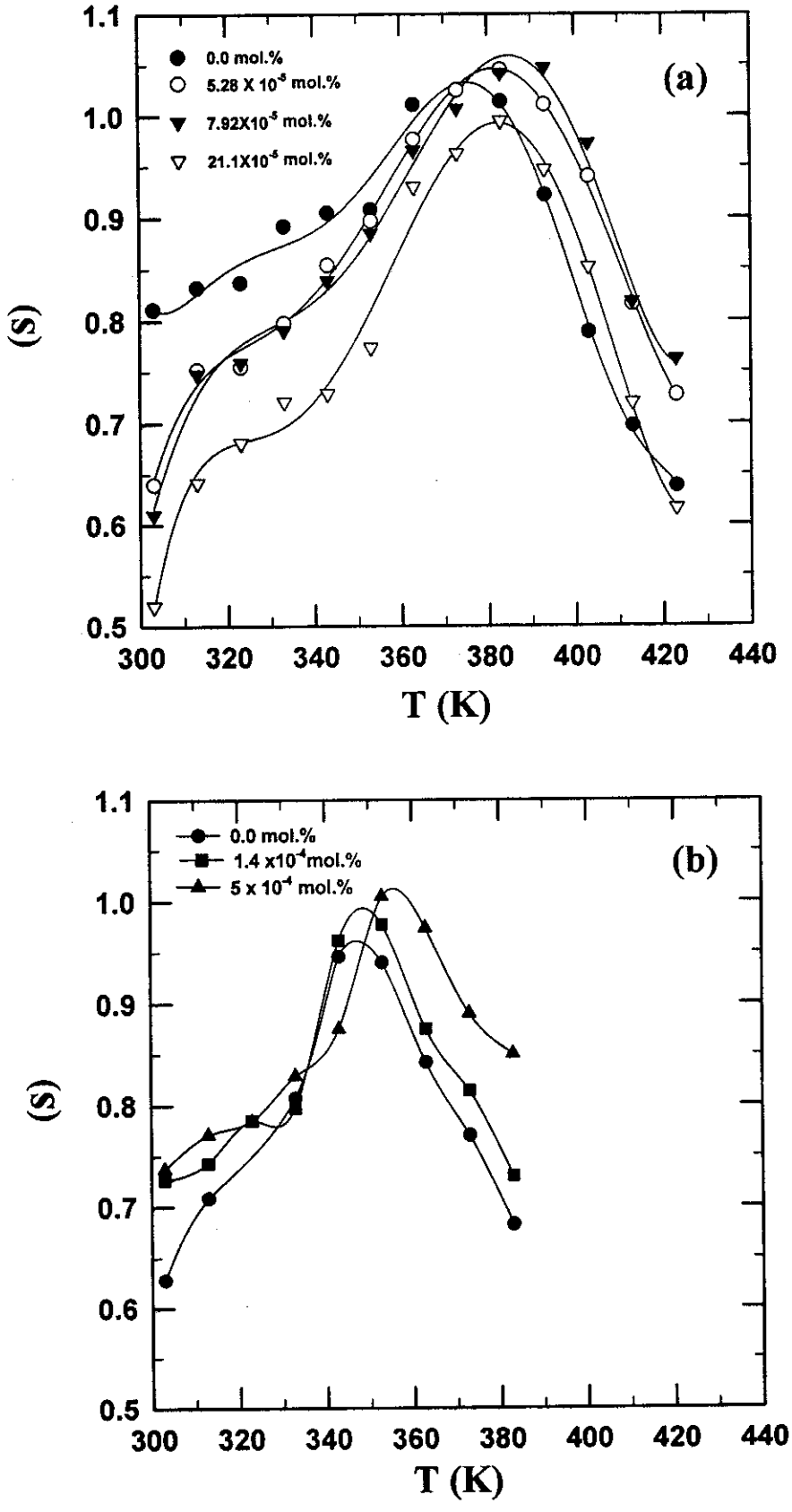

Fig.(IV.6) Temperature dependence of the exponent s for PMMA and PMMA/Perylene prepared by ,(a) thermal polymerization and (b)solvent casting methods.

samples at different fixed frequencies has been studied. Typical plot is given in Fig. (IV.7) as a representative diagram for all samples investigated. It is noted that $\sigma_{tot.}(\omega)$ is thermally activated up to a certain value σ_p and then attenuates in agreement with the behavior observed in dc conductivity measurements. The activated part in $(\sigma_{tot.}(\omega).-10^3/T)$ relation could be discussed according to Arrhenius relation described before. The values of the activation energy ΔE_{ac} are obtained at different frequencies and listed in Table (IV.6). It is observed that,

1-The activation energy for thermally prepared samples increases by increasing dye content in contrast to solvent cast samples.

2-The peak conductivity σ_p for thermally prepared samples appears in a temperature range higher than that of solvent cast samples. The comparison between σ_{dc} and $\sigma_{tot.}(\omega)$ showed the following characteristics:

- The values of ac conductivities are higher than those of dc.
- The values of ac activation energies are lower than those of dc.
- By increasing the applied field frequency on the samples the value of σ_p shifts toward higher temperatures, this because the increase of the applied field frequency enhances the carrier jumping and subsequently the conductivity. This leads to the shift of the peak to higher temperature.

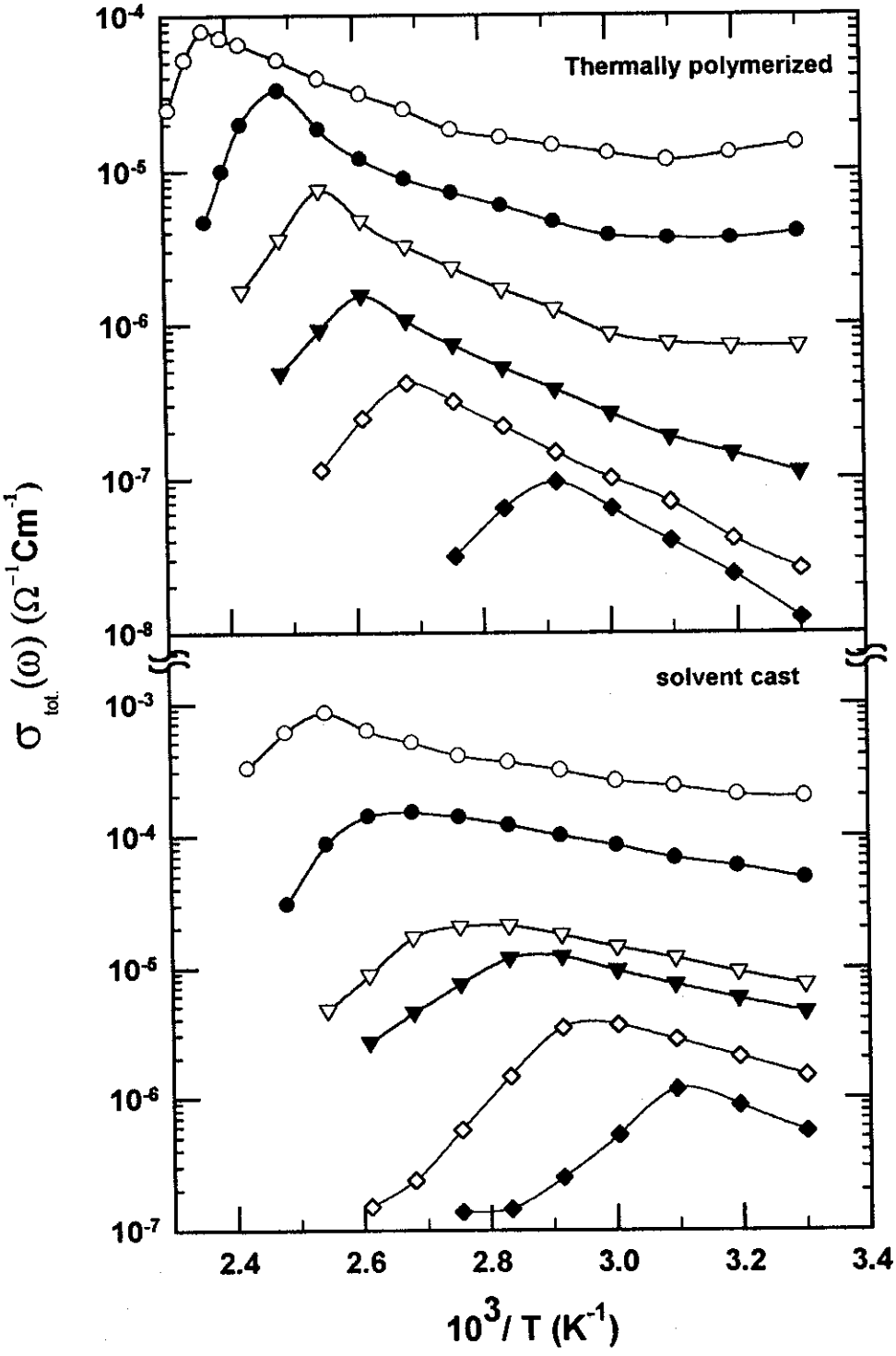

Fig.(IV.7) Temperature dependence of the total conductivity, $\sigma_{tot}(\omega)$, for pure PMMA samples at field frequencies (—◆—) 1 kHz, (—◇—) 10 kHz, (—▼—) 50 kHz, (—▽—) 100 kHz, (—●—) 500 kHz and (—○—) 1 MHz.

Table(IV.6): The calculated values of ac activation energy, ΔE_{ac}, at different frequencies for (PMMA/perylene) samples.

Concentration mol. %	1 kHz	10 kHz	50 kHz	100 kHz	500 kHz	1MHz
Thermally polymerized						
0.00	0.45	0.39	0.33	0.27	0.21	0.17
6.33×10^{-5}	0.51	0.43	0.35	0.31	0.25	0.21
7.92×10^{-5}	0.56	0.47	0.39	0.35	0.31	0.25
1.06×10^{-5}	0.61	0.52	0.48	0.41	0.36	0.29
1.37×10^{-4}	0.66	0.58	0.52	0.47	0.39	0.31
2.11×10^{-4}	0.72	0.63	0.57	0.50	0.43	0.36
Solvent Cast						
0.00	0.31	0.26	0.22	0.19	0.17	0.14
1.78×10^{-4}	0.25	0.21	0.18	0.17	0.15	0.12
5.00×10^{-4}	0.21	0.18	0.15	0.13	0.11	0.90

Section (C)

Dielectric Properties of PMMA/perylene

The dielectric properties ε', tanδ and ε" have been studied in the temperature range (303-433K) and frequency range (10^3-5x10^6 Hz). This study has two important features, the first is that the physical properties exhibited by Poly(acrylate) family in industrial applications are significantly influenced by the presence of relaxation transitions (α and β tranitions). These transitions are low energy transitions and often occur over a narrow temperature range. Therefore, analyzing these transitions requires a technique that offers high sensitivity and good resolution, dielectric analysis can provide both of these capabilities. The second is that a necessary requirement for FSCs applications is a large Stokes shift which is known to be a function of the dielectric permittivity ε' and the refractive index (n)

(IV.C.1) Dielectric Permittivity

Fig.(IV.8) illustrates the frequency dependence of the dielectric permittivity ε' for thermally polymerized and solvent-cast pure PMMA samples at different temperatures. For cast polymer a reduction in ε' by increasing frequency occurs in three stages where as it occurs in two stages in the case of thermally polymerized sample. This behaviour can be described by the Debye dispersion relation [108],

$$\varepsilon' = \varepsilon'_{\infty} + \frac{(\varepsilon'_s - \varepsilon'_{\infty})}{1+\omega^2\tau^2} \qquad \text{(IV-6)}$$

where, ε` is the dielectric permittivity at angular frequency ω, ε'_s is the

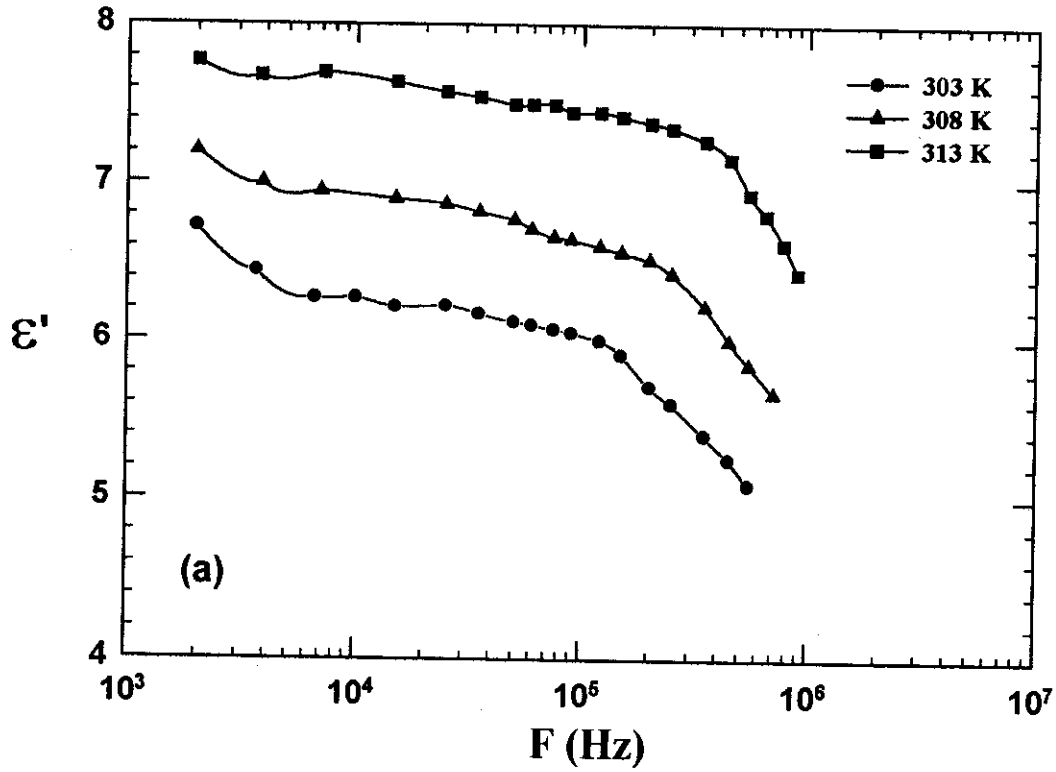

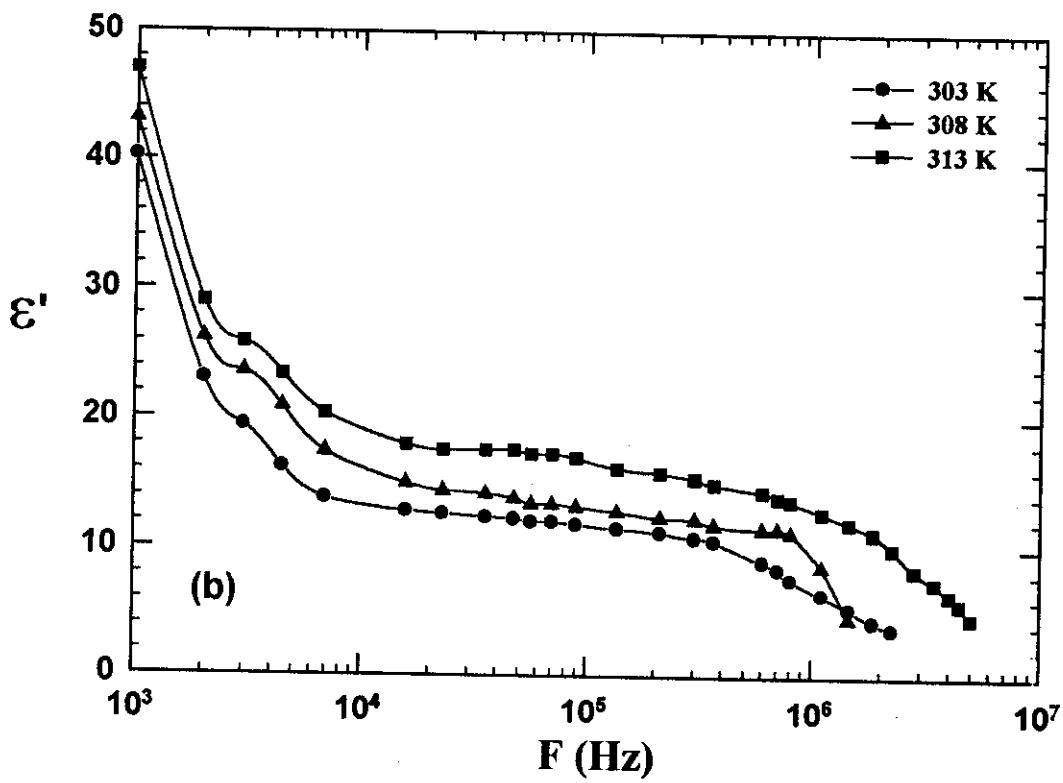

Fig.(IV.8) Frequency dependence of the dielectric permittivity, ε', for pure PMMA samples, (a) thermally polymerized and (b) solvent cast.

static dielectric permittivity, ε'_{∞} is the infinite dielectric permittivity and τ is the dielectric relaxation time.

In the first stage (for solvent cast sample), the high values of dielectric permittivity can be attributed to the interfacial polarization effects due to discontinuity of the dielectric medium as a result of the presence of solvent. This is expected because of the acidic nature of solvent which leads to accumulation of charges at the polymer- solvent interface [107,146]. In the second stage, the recorded mild attenuation of ε' by increasing frequency for both cases (thermally and solvent cast samples) can be attributed to orientational polarization of the main chain segments. In addition the remarkable decreases of ε' at high frequency range can be attributed to the lag of dipole orientation by increasing frequency. In the case of solvent cast sample the rate of attenuation of ε' is more pronounced because of the higher mobility of acrylate group in the presence of solvent molecules.

The temperature dependence of ε' is shown in Fig. (IV.9) for pure PMMA samples, the trend of ε' (T) is typical for a polar dielectric [107,141]. By increasing temperature the orientation of acrylate group increases and ε' increases up to a maximum and then drops at a certain temperature, this drop in ε' can be attributed to the intensified thermal oscillations of the polymer which disturb the orderliness of their orientations. It is clear that the solvent cast sample has comparatively higher values of ε' and exhibits a high temperature gradient $\partial\varepsilon'/\partial T$ compared with thermally polymerized sample, which reflects the strong polar nature of the solvent cast sample than the thermally polymerized one.

The frequency and temperature dependence of ε' for perylene

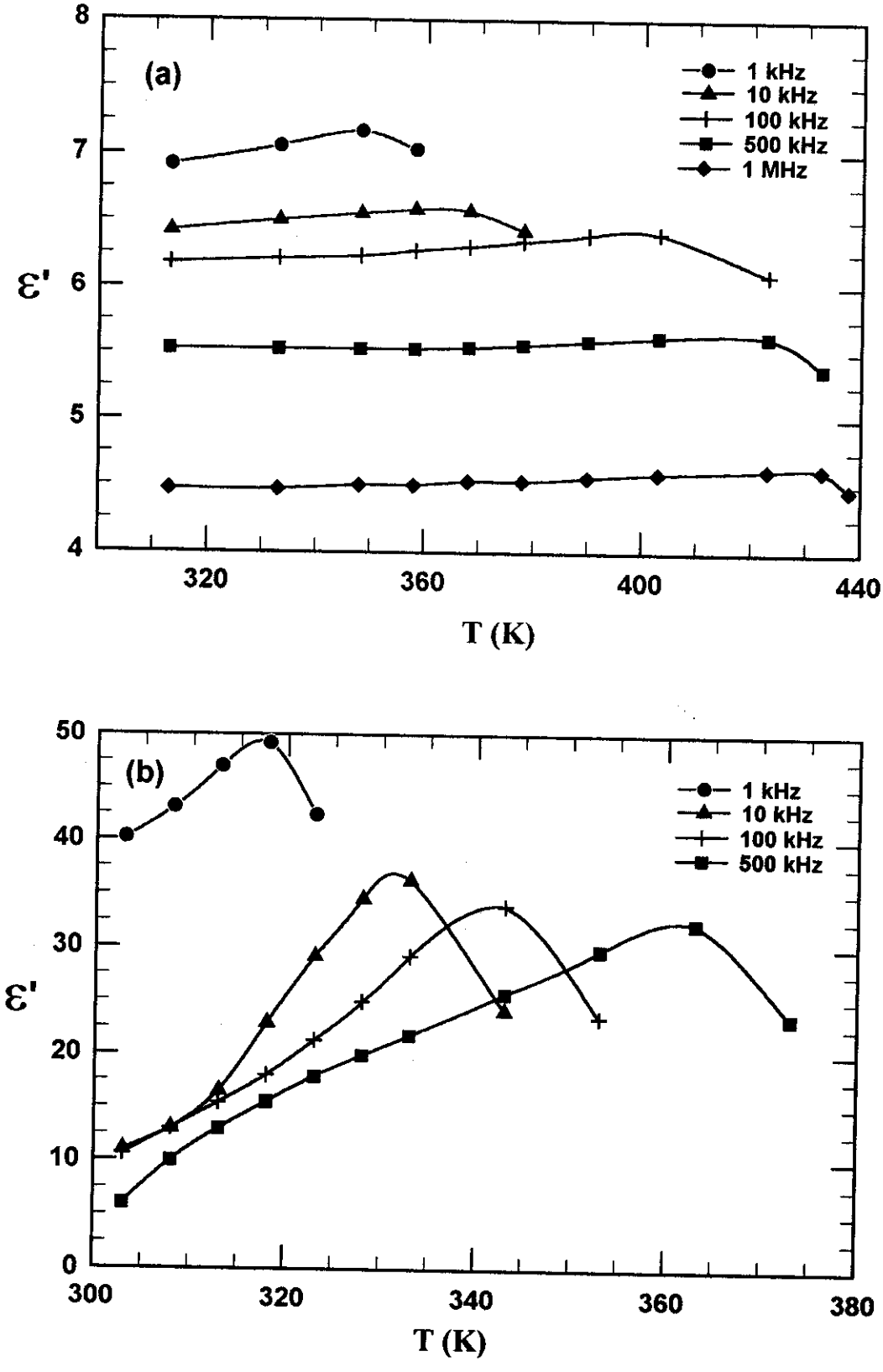

Fig.(IV.9) **Temperature dependence of the dielectric permittivity , ε', for pure PMMA samples , (a) thermally polymerized and (b) solvent cast.**

doped PMMA samples have been studied and showed the same behaviour of the pure samples. Fig.(IV.10) shows the concentration dependence of ε'. It is also noted that ε' decreases by increasing dye concentration for thermally prepared samples whereas it increases by increasing dye concentration in the case of solvent cast samples. These results are in agreement with the conductivity measurements, since the conductivity of a real dielectric is directly related to the dielectric permittivity [147].

(IV.C.2) Dielectric Loss

The frequency dependence of tan δ was studied for PMMA samples and is represented in Fig. (IV.11), which represents a typical plot for all PMMA/perylene samples. It is clear that each tan δ (F) curve show two maxima at certain frequencies, both maxima shift downward right towards higher frequency range by increasing temperature. For solvent cast sample it is noted that the values of tan δ peaks are lower than those of thermally prepared sample. In addition the maxima of tanδ (F) appear in higher frequency range comparing with thermally prepared sample. This is a result of the difference in T_g of both samples. The lower T_g (in the solvent cast sample) decreases the polymer viscosity and subsequently the dipole relaxation time [26].

The higher values of tan δ for thermally prepared samples than that of solvent cast samples means the higher energy dissipation due to the fact that the dipoles are stiffly attached to the main chain. This confirms our discussion in the previous sections.

The attenuation of tan δ peak by increasing temperature or frequency observed in Figs. (IV.11, 12) can be attributed to the phonon

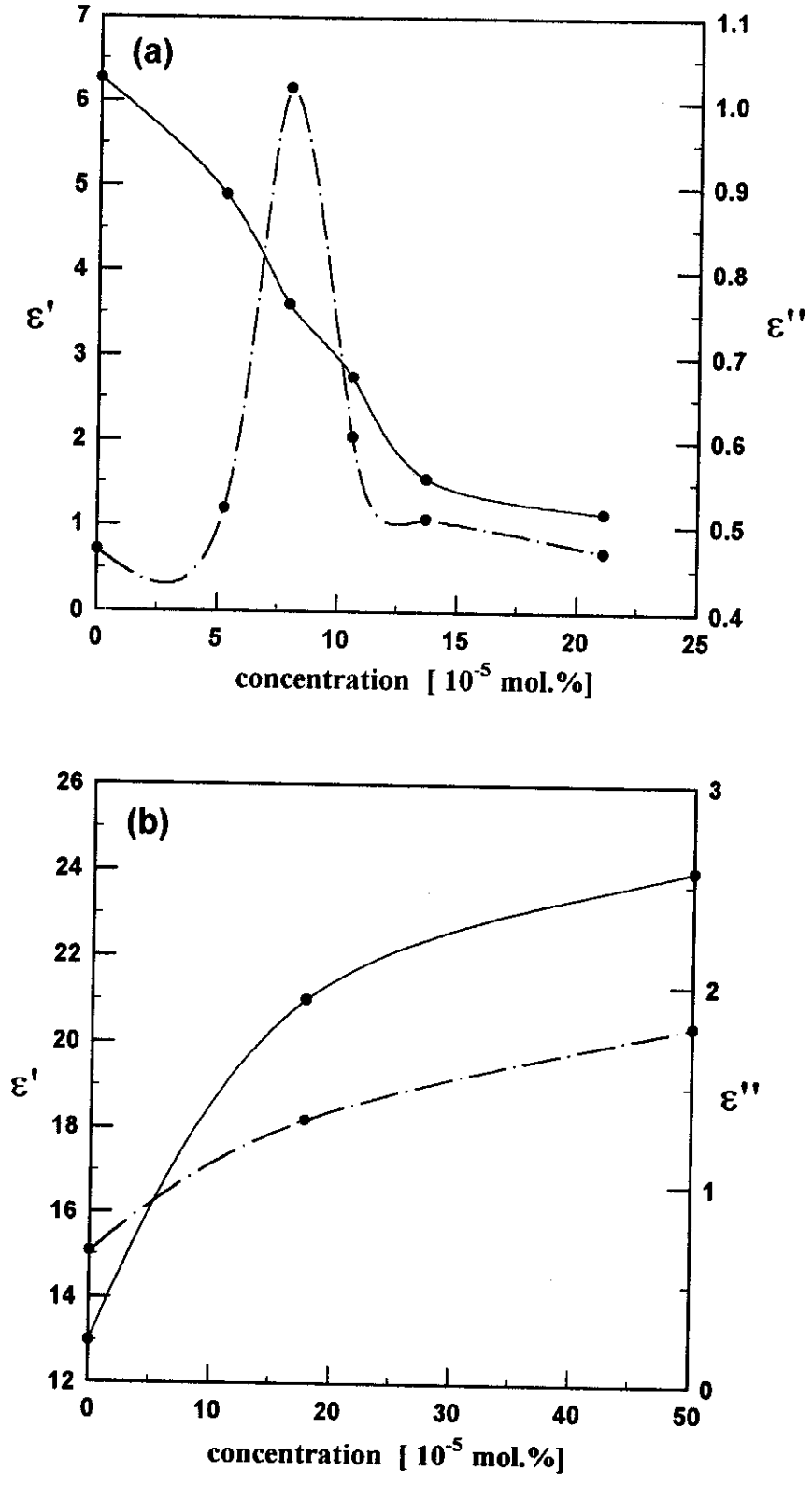

Fig.(IV.10) Effect of perylene concentration on the dielectric permittivity ε' (——) and the dielectric loss ε'' (- - - -) for (a) thermally polymerized and (b) solvent cast for PMMA/perylene samples at temperature, 300 K and frequency 500 Hz.

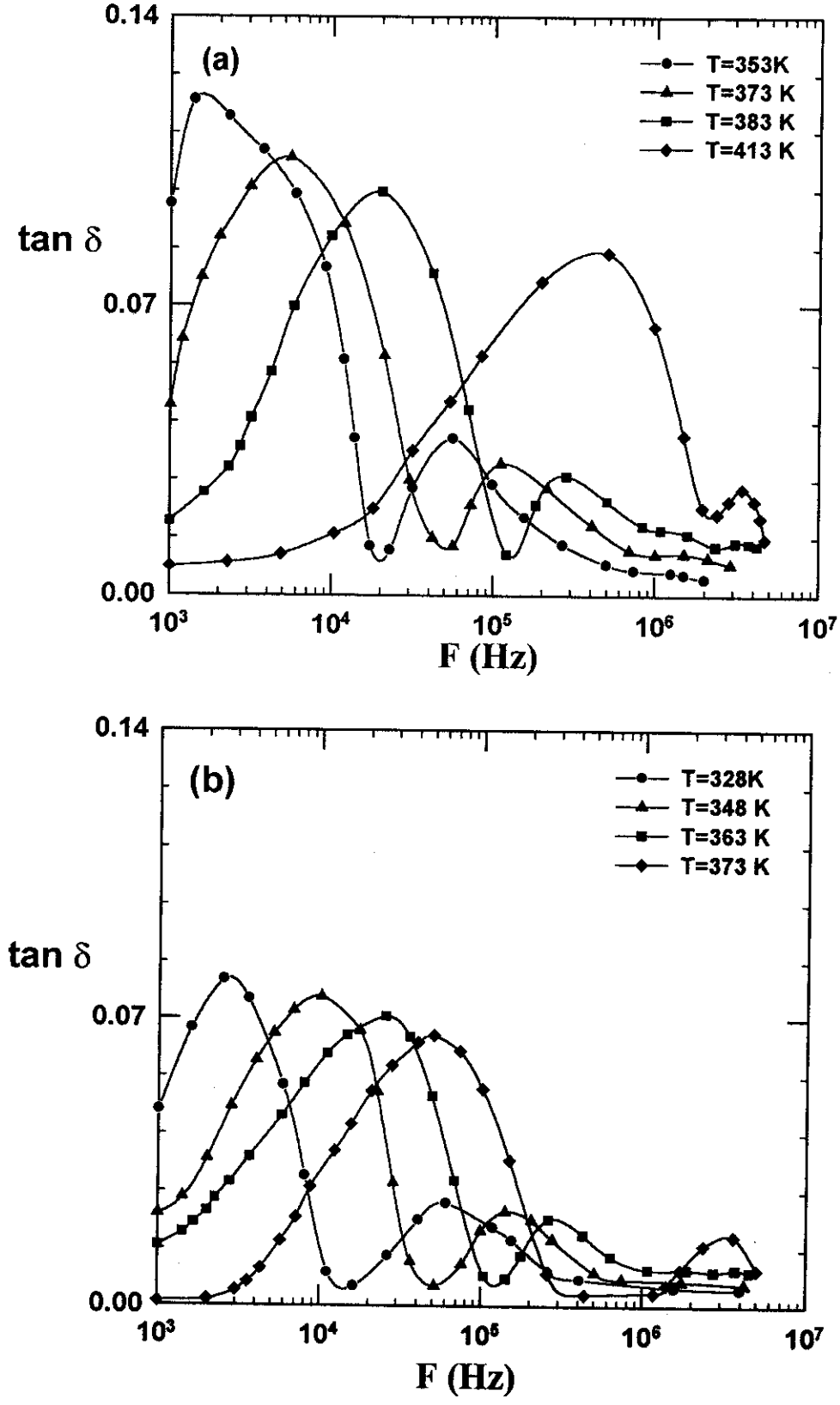

Fig.(IV.11) Frequency dependence of the loss tanget,tanδ, for pure PMMA samples (a) thermally polymerized and (b) solvent cast.

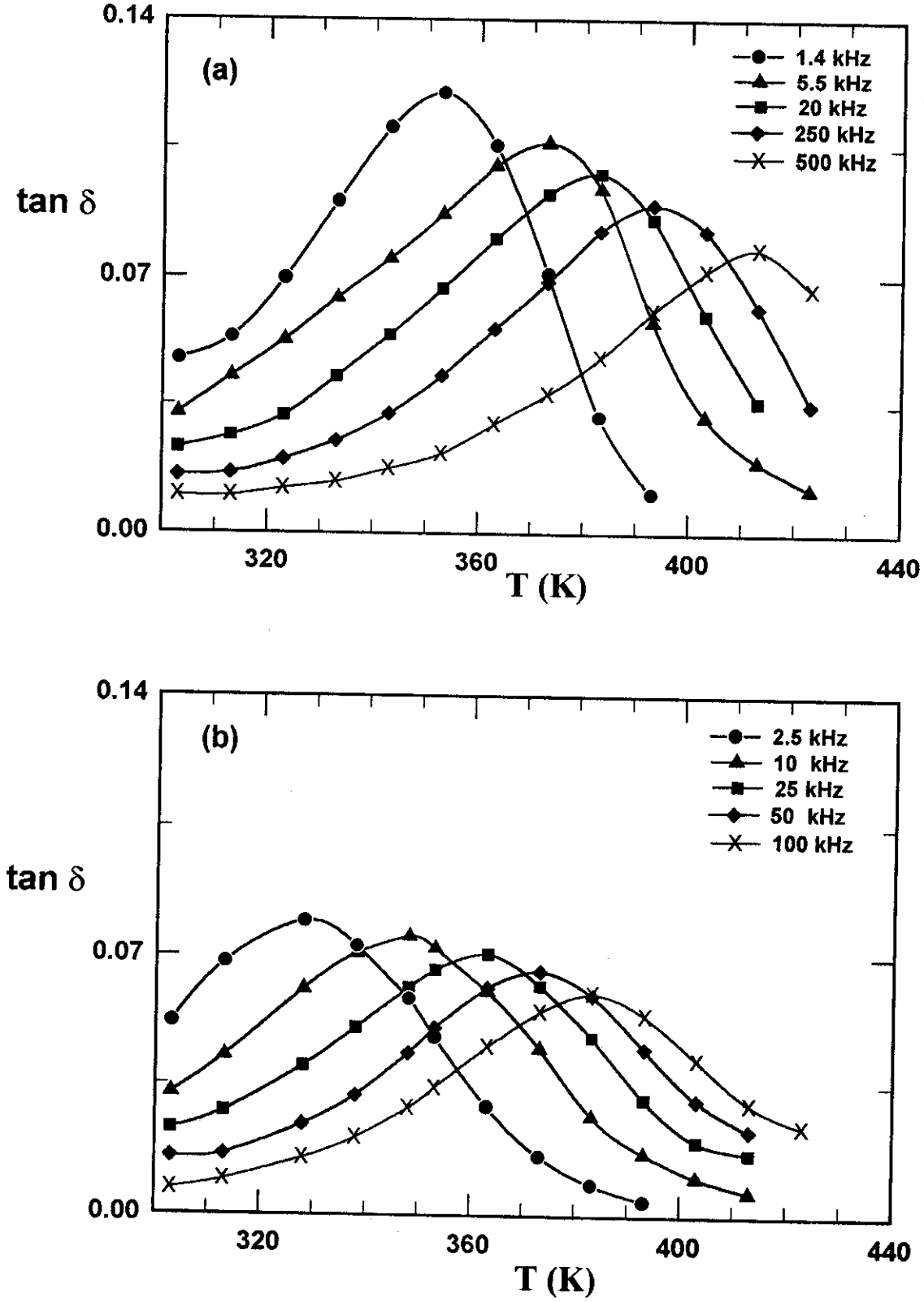

Fig.(IV.12) Temperature dependence of the loss tangent, tanδ, for pure PMMA samples, (a)thermally polymerized and (b)solvent cast.

dipole interaction which leads to a lowering of the energy transfered to the dielectric medium. This behaviour characterizes amorphous polymers [107].

Fig.(IV.13) shows the frequency dependence of ε" at fixed temperatures for pure PMMA samples, which represent a typical plot of all the investigated samples. Two peaks in the dispersion relation are observed. The first appears at low frequency and is associated with orientation of chain sections consisting of large number of monomeric units (segments)[109]. In PMMA this is referred to the motion of acrylate group about C-C bond and results from large-scale conformational rearrangements of the polymer chain backbone [37,148]. The mechanism can occur by the hindered rotation of the acrylate groups around main chain bonds. The motion of acrylate group about two colinear C-C bonds can be explained as crankshaft rotation [106,149]. This relaxation occurs under the conditions where segmental motion is possible (above T_g of the polymer) and referred to as α–relaxation (glass-rubber transition). The second peak appears at high frequency is associated with the rotation of ester side group about the C-C bond which links it to the main chain. Losses of this kind almost occur below T_g and sometimes occur above T_g referring to the β-relaxation [109] (glass – glass transition).

It is clear that ε''_{max} (F) is much higher for dipole segmental loss than dipole group loss. This can be attributed to the fact that the ester side groups are more mobile kinetic units than the acrylate group loss. due to the strong polar nature of the former than that of the later. In solvent cast sample the two relaxations are significantly shifted downward right towards higher frequencies at lower temperatures. This

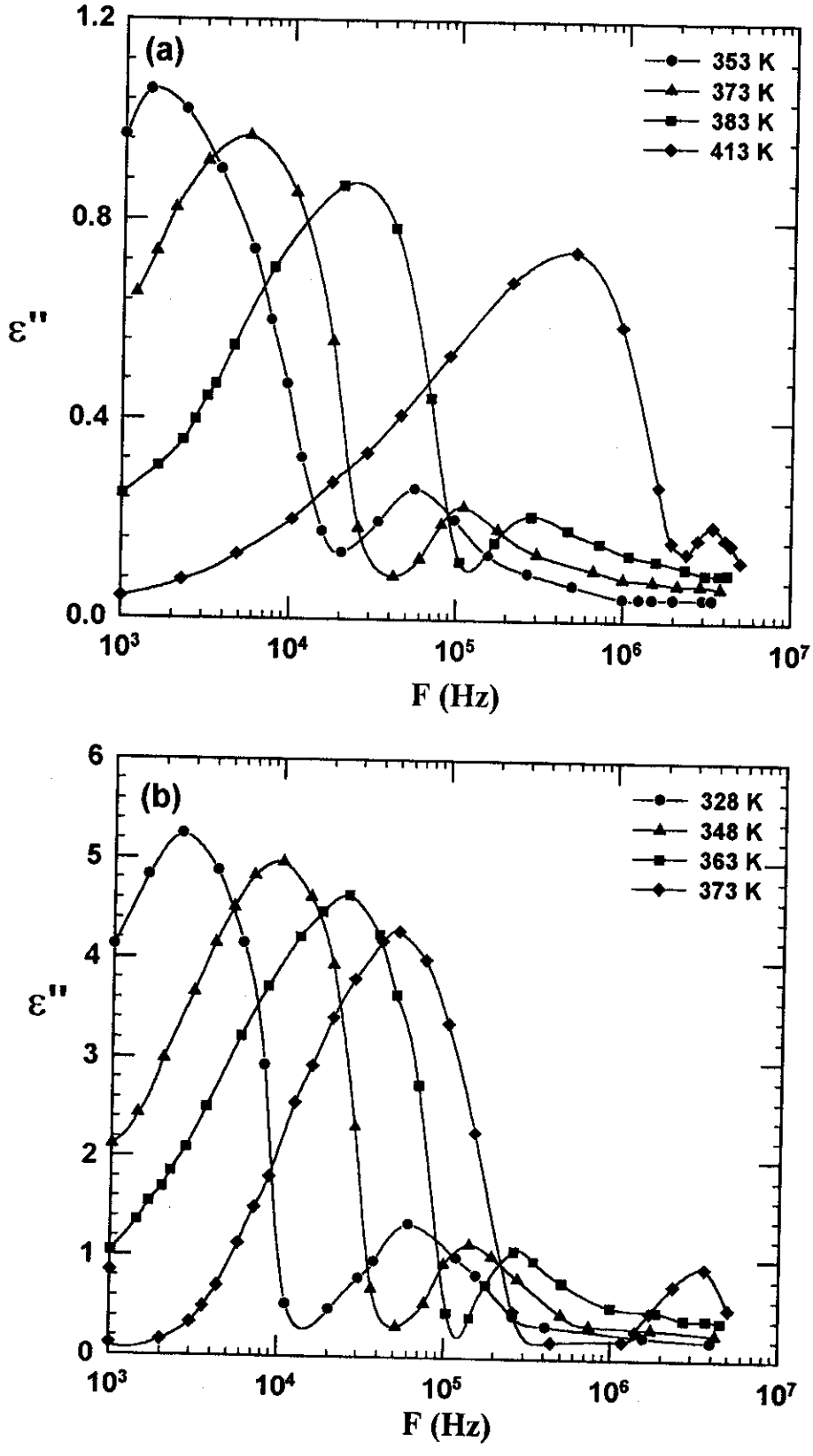

Fig.(IV.13) **Frequency dependence of the dielectric loss , ε'', for pure PMMA samples, (a) thermally polymerized and (b) solvent cast.**

shift can be explained by the plastizing effect induced by the presence of solvent molecules between the PMMA main chains[36,37], by which the dipoles need less energy to move.

Fig. (IV.14) shows the temperature dependence of ε" at different frequencies for the pure PMMA samples. Only a single peak in ε" (T) curves is observed which position depends on the frequency of the applied field. By increasing frequency the position of ε''_{max}.(T) shifts downward right towards higher temperatures. The explanation for the appearance of this peak loss in ε"(T) curves can be ascribed to the fact that the β-process is much broader than the α-process. This is due to the fact that the local barriers to rotation of the side groups are different along the chain as a consequence of the irregularity of the vitreous state [150]. In the contour map described in literatures [151,152], α and β processes are only well separated below 1 kHz. So ε''_{max}(T) can be ascribed to an α β process in which the side groups cooperate with the back bone motions in a micro brownian motion which has properties similar to a pure α-process [153-155].

Fig.(IV.10) shows the effect of dye concentration on ε" for thermally and solvent cast samples. It is noticed that ε" increases by increasing dye concentration for low dye concentrations in thermally prepared samples and all the solvent cast samples. The increase in ε"can be explained by the following,

- The non-polar nature of the dye molecules reduces the polarization process and causes the shift of the (α and β) relaxations to lower frequencies.

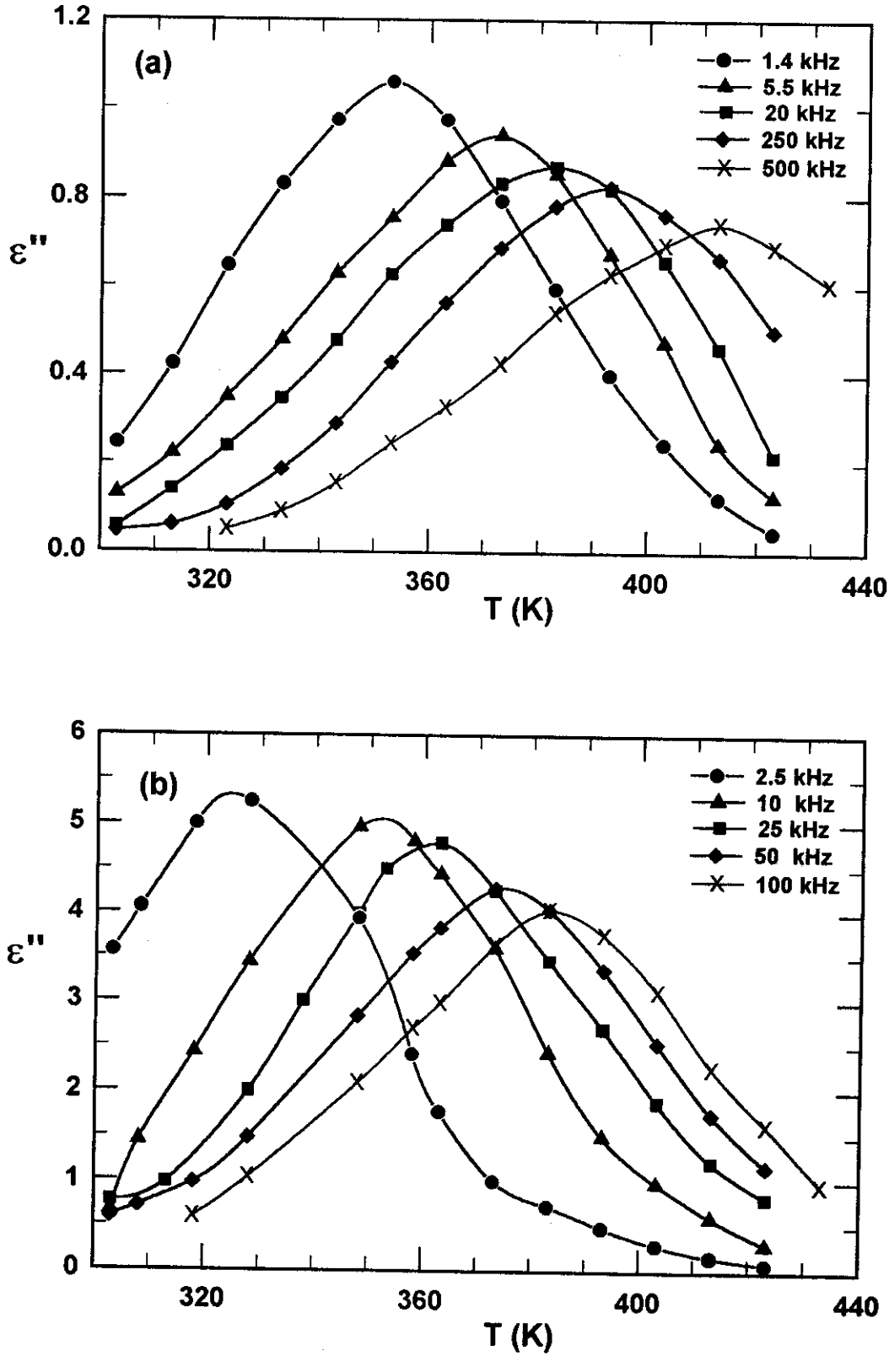

Fig.(IV.14) Temperature dependence of the dielectric loss , ε'', for pure PMMA samples ,(a) thermally polymerized and (b) solvent cast.

♦ The large size and bulky nature of the dye molecules increase the steric hindrance to the motion of the dipoles (in case of thermally prepared polymer). In the case of solvent cast samples this effect cause the trapping of solvent between chains and subsequently increasing the intermolecular interactions discussed before.

For dye concentrations higher than 7.92×10^{-5} mol.% in the thermally polymerized samples, these factors are opposed by the increase of the free volume and chain mobility caused by the aggregation of dye molecules.

(IV.C.3) Relaxation Time

Investigation of the frequency or temperature dependence of the dielectric loss factor enables an estimate of the relaxation time of the orientation moment in the (α and β relaxations). Making use of the relation [110],

$$\omega_{max} \cdot \tau = 2\pi f_{max} \tau = 1 \qquad \text{(IV-7)}$$

where f_{max} is the linear field frequency at which ε'' passes through a maximum and τ is the relaxation time. The values of f_{max} can be shown in Tables (IV.7,8) for the dipole segmental and dipole group losses respectively.

The obtained values of relaxation times τ_1 and τ_2 corresponding to the dipole segmental and dipole group losses are plotted against dye concentration as shown in Fig. (IV.15). It is observed that the relaxation times for thermally polymerized samples increase by increasing dye concentration and pass through a maximum at the concentration 7.92×10^{-5} mol.% for both types of relaxations. While they increase by

Table(IV.7):The obtained values of the peak frequency, f_{max} (Hz) corresponding to the dipole segmental loss for PMMA/perylene samples.

(a) Thermally polymerized.

T (K)	0.00 mol .%	$6.33x10^{-5}$ mol .%	$7.92x10^{-5}$ mol .%	$1.06x10^{-4}$ mol.%	$1.37x10^{-4}$ mol .%	$2.11x10^{-4}$ mol .%
353	$1.4x10^{3}$	$1.3x10^{3}$	$1.1\ x10^{3}$	$1.2\ x10^{3}$	$1.5\ x10^{3}$	$1.6\ x10^{3}$
373	$5.5x10^{3}$	$4.0x10^{3}$	$4.0\ x10^{3}$	$5.0x10^{3}$	$7.0x10^{3}$	$7.5\ x10^{3}$
383	$2.0x\ 10^{4}$	$1.0x10^{4}$	$8.0x10^{3}$	$1.0x10^{4}$	$2.0x10^{4}$	$5.0\ x10^{4}$
393	$2.5x10^{5}$	$1.0x10^{5}$	$8.0x10^{4}$	$1.6\ x10^{5}$	$3.5x10^{5}$	$6.0\ x10^{5}$
413	$5.0x10^{5}$	$4.0x10^{5}$	$2.0\ x10^{5}$	$3.0\ x10^{5}$	$6.0\ x10^{5}$	$8.5\ x10^{5}$

(b) Solvent cast

T(K)	0.00 mol. %	$1.78x10^{-4}$ mol. %	$5.00x10^{-4}$ mol. %
328	$2.5\ x10^{3}$	$1.4\ x10^{3}$	$1.0\ x10^{3}$
348	$1.0\ x10^{4}$	$7.5\ x10^{3}$	$3.0\ x10^{3}$
363	$2.5\ x10^{4}$	$2.0\ x10^{4}$	$1.5\ x10^{4}$
373	$5.0\ x10^{4}$	$4.0\ x10^{4}$	$3.0\ x10^{4}$
383	$1.0\ x10^{5}$	$8.0\ x10^{4}$	$7.0\ x10^{4}$

Table(IV.8):The obtained values of the peak frequency, f_{max} (Hz) corresponding to the dipole group loss for PMMA /perylene samples.

(a) Thermally polymerized.

(K)	0.0 mol.%	$6.33x10^{-5}$ mol.%	$7.92x10^{-5}$ mol.%	$1.06x10^{-4}$ mol.%	$1.37x10^{-4}$ mol.%	$2.11x10^{-4}$ mol.%
53	$5.6x10^4$	$5.0 x10^4$	$3.6 x10^4$	$3.8 x10^4$	$4.0 x10^4$	$5.8 x10^4$
73	$1.1 x10^5$	$1.0 x10^5$	$1.0 x10^5$	$1.1x10^5$	$1.2 x10^5$	$1.5 x10^5$
33	$2.8 x10^5$	$2.2 x10^5$	$2.4 x10^5$	$2.6 x10^5$	$3.0 x10^5$	$8.5 x10^5$
93	$1.3 x10^6$	$1.0 x10^6$	$4.4 x10^5$	$4.6 x10^5$	$5.2 x10^5$	$2.0x10^6$
.3	$3.4 x10^6$	$3.0 x10^6$	$1.0 x10^6$	$1.2x10^6$	$2.7x10^6$	$3.8x10^6$

(b) Solvent cast

T(k)	0.0 mol.%	$1.78x10^{-4}$ mol.	$5x10^{-4}$ mol.%
328	$6.0 x10^4$	$5.0 x10^4$	$2.0 x10^4$
348	$1.4 x10^5$	$1.2 x10^5$	$8.0 x10^4$
363	$2.6 x10^6$	$1.6 x10^6$	$1.0 x10^5$
373	$3.6 x10^6$	$2.4 x10^6$	$1.0 x10^6$
383	$4.2 x10^6$	$3.4 x10^6$	$1.5 x10^6$

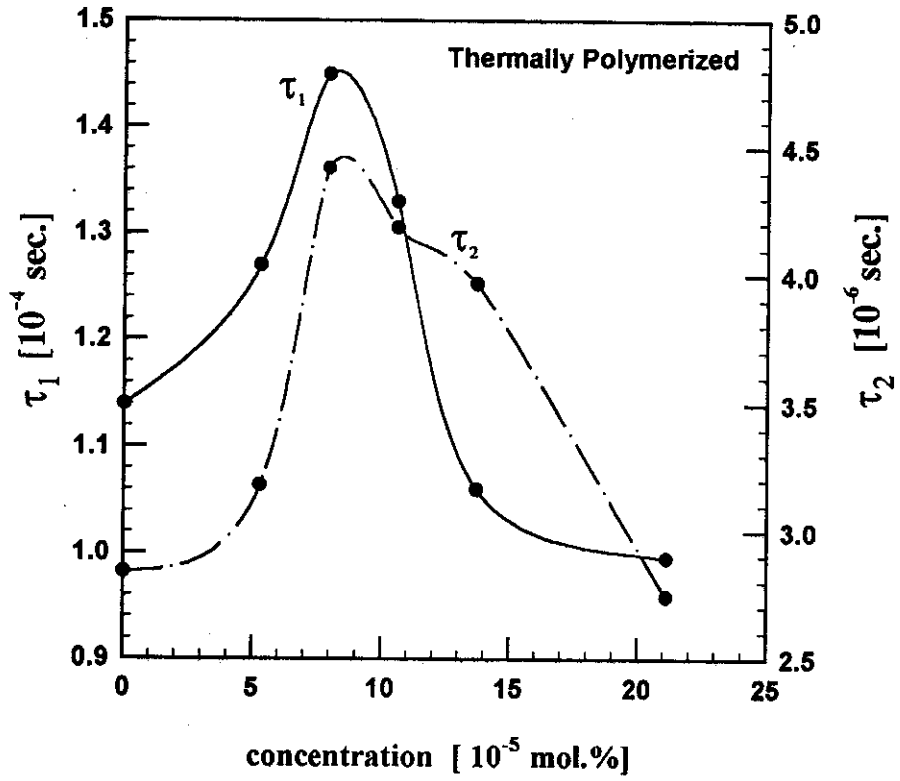

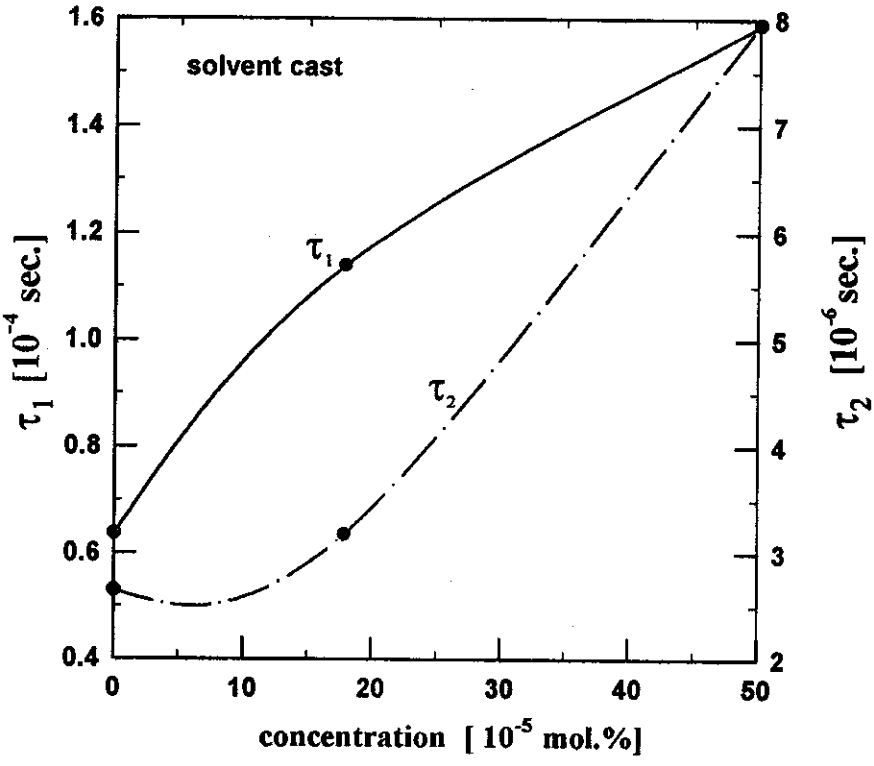

Fig.(IV.15) Effect of perylene concentration on the relaxation times (τ_1 and τ_2) corresponding to the dipole segmental and dipole group relaxations in PMMA /perylene samples , at 353 K for thermally polymerized and 328 K for solvent cast samples.

increasing dye concentration for solvent cast samples. This behaviour confirms the explanation given in discussing ε" behaviour.

The obtained relaxation time ($\tau=1/\omega_{max}$), which shows an attenuation with increasing temperature, obeys an exponential relation of the from [111,156],

$$\tau = (h/kT) \exp(\Delta G/RT) \qquad \textbf{(IV-8)}$$

where Δ G is the free energy of activation for dipole relaxation, which is related to the enthalpy Δ H and entropy ΔS of activation by the relation ;

$$\Delta G = \Delta H - T\,\Delta S \qquad \textbf{(IV-9)}$$

It follows from equation (IV-8) that

$$\Delta G = RT \ln\left[\frac{kT\tau}{h}\right] \qquad \textbf{(IV-10)}$$

A semi-logarithmic plot of ln T τ versus $10^3/T$ is shown in Fig. (IV.16) for pure PMMA samples as a representative figure for all samples. The values of ΔG, ΔH and ΔS are obtained for all investigated samples and listed in Tables (IV.9, 10). The effect of the sample preparation and dye concentration on the thermodynamic parameters for the dipole segmental and dipole-group relaxations is observed. In case of thermally prepared samples both ΔH and ΔS reach its minimum at concentration of 7.92×10^{-5} mol.% and then increase by increasing the dye content. While in the case of solvent cast samples Δ H and Δ S increase by increasing dye content, this can be understood on the following basis. In the case of thermally prepared samples the dye fills the voids in the polymer structure (only for low concentration). For higher dye concentrations, the dye plays an important role for rearranging the polymer structure; (see

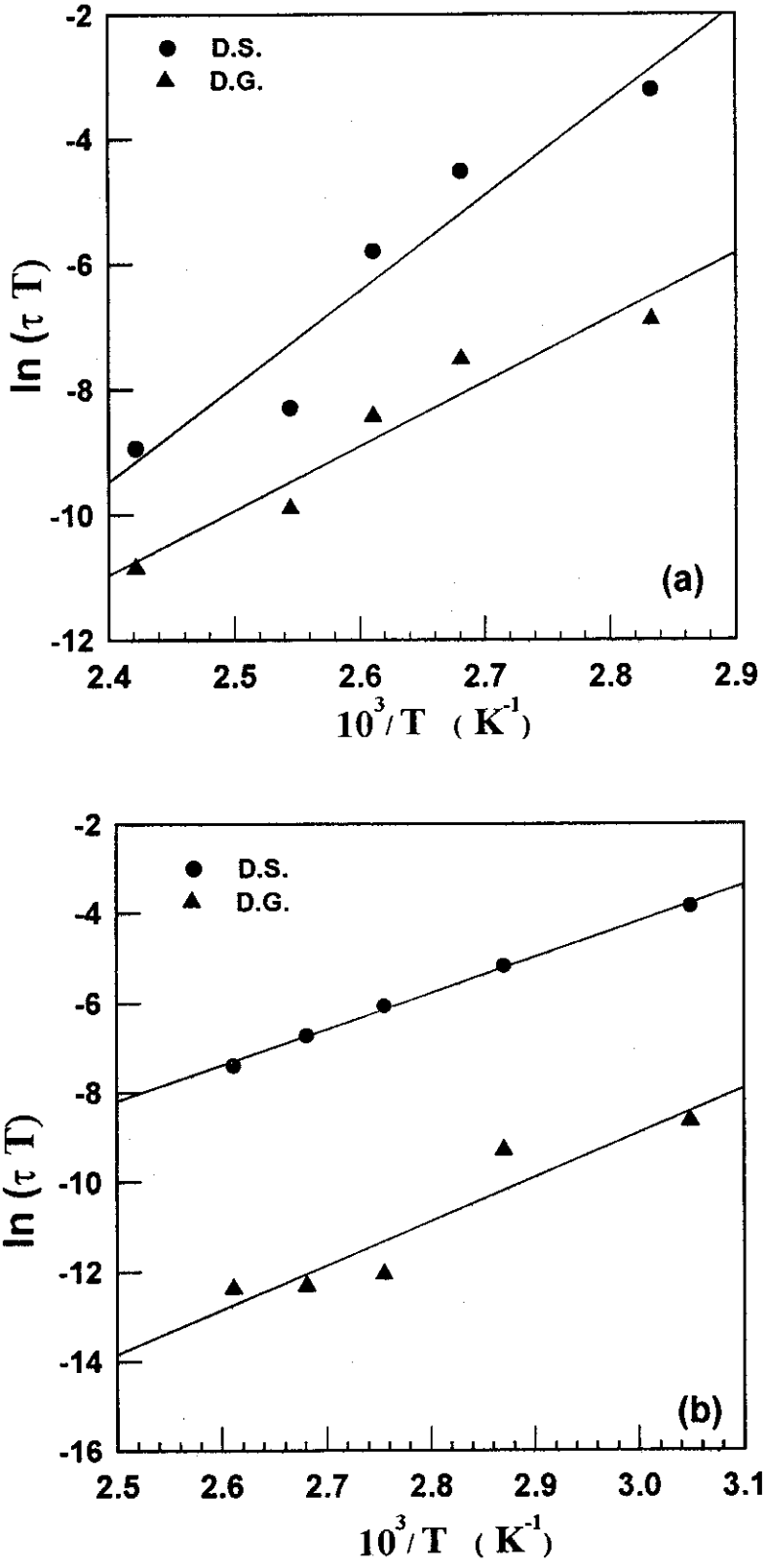

Fig.(IV.16) Temperature dependence of the relaxation times for the dipole segmental D.S. and dipole group D.G. losses in pure PMMA (a) thermally polymerized and (b)solvent cast.

Table (IV.9): The thermodynamic parameters corresponding to the dipole segmental loss, for PMMA/perylene samples.

(a) Thermally polymerized

Concentration mol. %	ΔG (353K) kJ/mol.	ΔH kJ /mol.	ΔS JK^{-1}/mol.
0.00	65.69	126.63	173.00
$6.33x10^{-5}$	66.68	124.50	164.00
$7.92x10^{-5}$	66.40	109.10	121.00
$1.06x10^{-4}$	66.14	117.46	145.00
$1.37x10^{-4}$	65.50	129.33	181.00
$2.11x10^{-4}$	65.30	137.85	206.00

(b) Solvent cast

Concentration mol. %	ΔG (328K) kJ/mol.	ΔH kJ/mol.	ΔS JK^{-1}/mol.
0.00	59.26	66.32	21.52
$1.78x10^{-4}$	60.84	73.04	37.20
$5.00x10^{-4}$	61.76	79.38	53.72

Table(IV.10): The thermodynamic parameters corresponding to the dipole group loss, for PMMA/perylene samples.

a) Thermally polymerized

Concentration mol. %	ΔG (353K) kJ/mol.	ΔH kJ/mol.	ΔS JK^{-1}/mol.
0.00	54.87	85.55	86.91
$6.33x10^{-5}$	55.20	84.45	82.86
$7.92x10^{-5}$	56.16	66.32	28.78
$1.06x10^{-4}$	56.00	68.28	34.79
$1.37x10^{-4}$	55.85	81.46	72.55
$2.11x10^{-4}$	54.75	88.85	96.60

(b) Solvent cast

Concentration mol. %	ΔG (328K) kJ/mol.	ΔH kJ/mol.	ΔS JK^{-1}/mol.
0.00	50.59	82.08	96.01
$1.78x10^{-4}$	51.09	77.32	79.97
$5.00x10^{-4}$	53.59	79.69	79.57

DSC results). In the solvent cast samples the confined solvent and dye have an effective influence on the thermodynamic parameters in addition the activation energy ΔG is found to be slightly changed by increasing dye content for all samples. This indicates that the mechanism of relaxation is the same for all samples since the dye does not contribute to the relaxation process due to its non-polar nature.

Section (D)

Spectroscopic Properties and Optical Efficiency of PMMA/perylene FSCs

(IV.D.1) Optical Properties

The use of PMMA as a base matrix for FSC applications requires accurate knowledge of their optical constants over a wide range of wavelength. In addition analyzing the absorption edges provides valuable information about the electronic band structure and stability of these matrices.

The optical absorption of thermally polymerized and solvent cast PMMA and PMMA/perylene samples of concentrations (6.33×10^{-5} and 1.78×10^{-4} mol.%) respectively has been studied. The optical absorption spectra were recorded in the wavelength range (200-900 nm) and are shown in Fig. (IV.17). The spectra show two major peaks: first is observed around 5.6 eV characterizing $\pi - \pi^*$ absorption band of PMMA and the second appears at 3.05 eV which can be attributed to S_o–S_1 transition of the dye. The peak position of the main absorption band is given by [122],

$$\lambda_m = \frac{8mC}{h} \frac{L^2}{N+1} \qquad \text{(IV-11)}$$

where m is the electron mass, h is Planck's constant, C is the velocity of light, L is the chain length and N is the number of π electrons. Equation (IV-11) indicates that, to first approximation, the position of the absorption band is determined only by the chain length and by the number of π electrons. The values of the absorption coefficient α have been estimated in the mentioned wavelength. The optical parameters

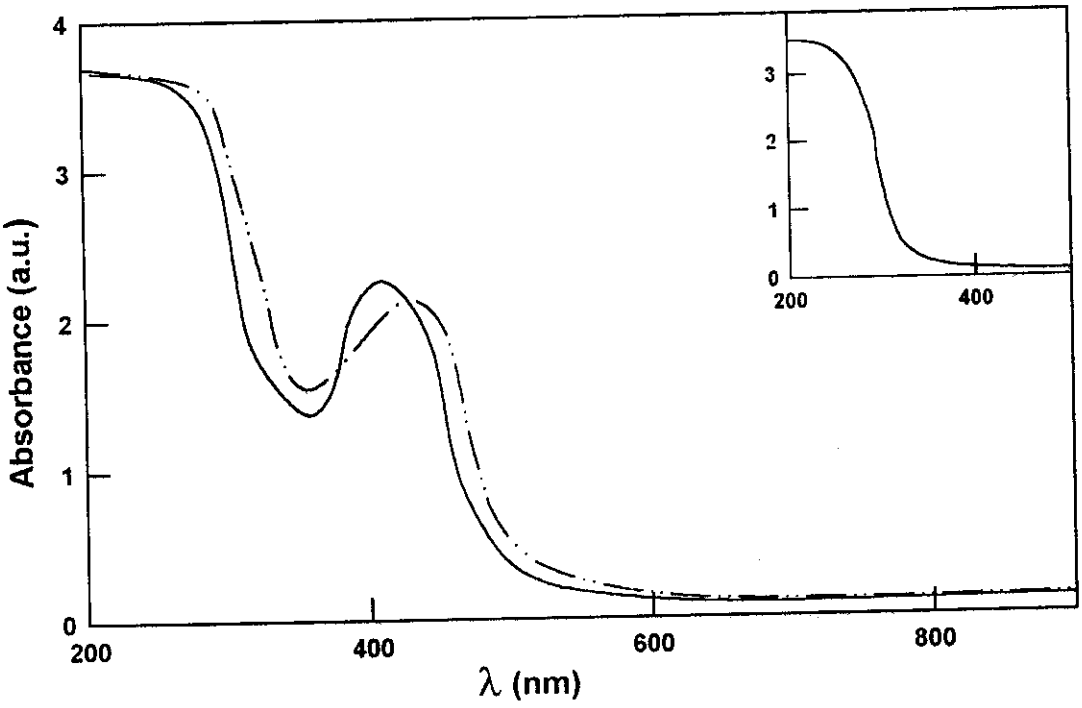

Fig.(IV.17.a) Optical absorption spectra for thermally polymerized PMMA (inset) and PMMA/perylene samples (——) before and (—··) after exposure to unfiltered light for 180 minutes.

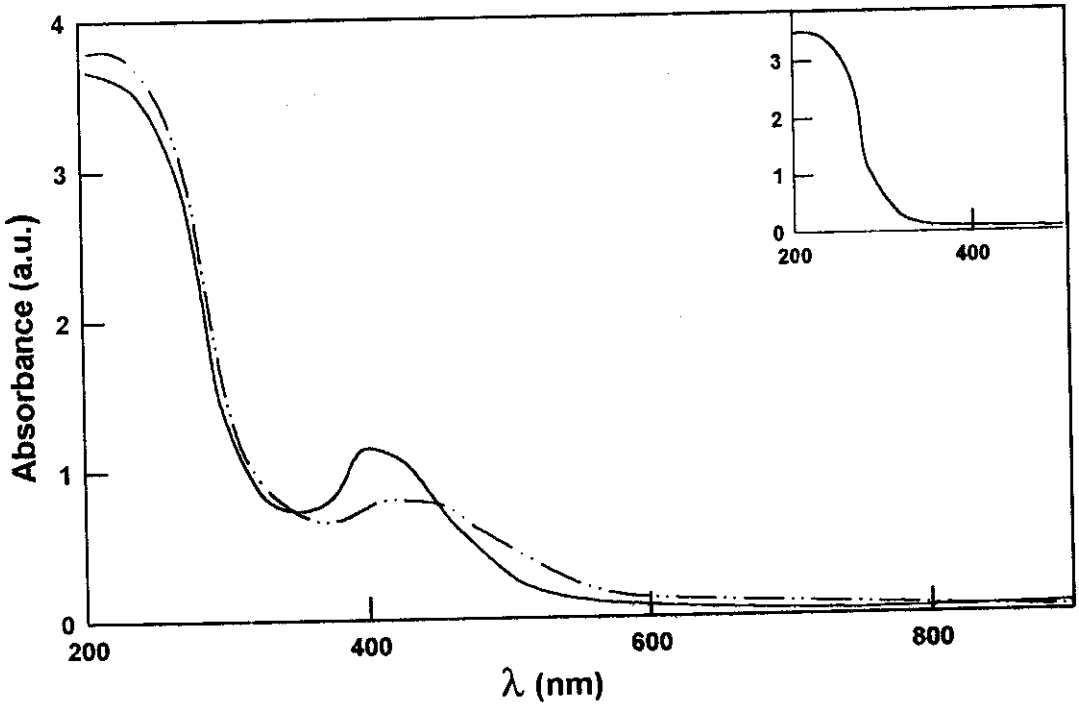

Fig.(IV.17.b) Optical absorption spectra for solvent cast PMMA (inset) and PMMA/perylene samples (——) before and (—··)after exposure to unfiltered light for 40 minutes.

were determined in the exponential region where $1 \leq \alpha \leq 10^4$ cm^{-1}.

Urbach[113] assumed that the absorption coefficient near the band edge shows exponential dependence on photon energy according to the following empirical relation [157,158]

$$\alpha = \alpha_o \exp (E/E_u) \qquad \text{(IV-12)}$$

where E_u is the Urbach's energy corresponding to the width of the band tails of the localized states in the band gap. These are formed as a result of extrinsic origins arising from defects or impurities, to extended states in the conduction band. The values of E_u were calculated by using the least square fitting of equation (IV-12). Figs.(IV.18,19) show the variation of $\ln\alpha$ vs E for the mentioned samples. It is observed that the absorption coefficient for solvent cast samples is higher than that for thermally polymerized. This may be due to a high transition probability of carriers across the corresponding small gap between the localized states [159]. Table (IV.11) shows that the value of E_u for solvent cast PMMA is higher than that of thermally polymerized. This is due to the presence of solvent, which is responsible for the formation of localized states in the band gap.

When a quantum of radiation is absorbed by a material the absorption coefficient as a function of photon energy ($E= h\nu$) for a simple parabolic band can be expressed by [160,161],

$$\alpha E \sim (E-E_g)^n \qquad \text{(IV-13)}$$

where n depends on the transition type and E_g is the optical gap. Figs (IV.18,19) show the dependence of $(\alpha E)^2$ on photon energy E which shows a linear behaviour that can be considered as evidence of the direct

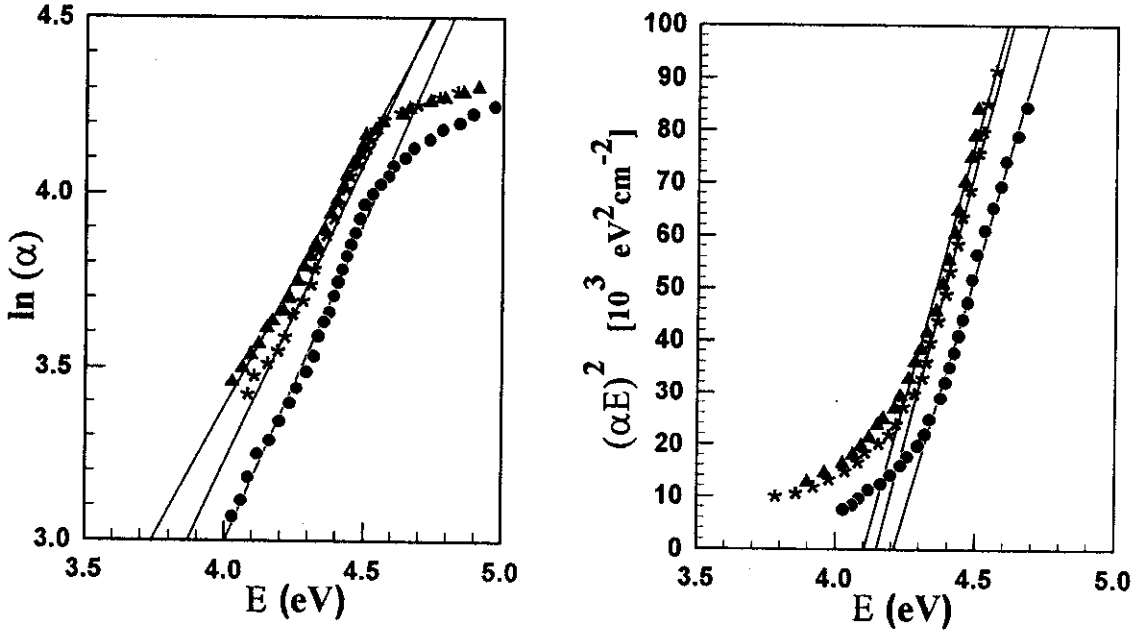

Fig.(IV.18) The dependence of ln (α) and $(\alpha E)^2$ on photon energy (E) for solvent cast PMMA /Perylene sample (•)befor and after exposure to unfiltered light (⋆)20 and (▲)40 minutes.

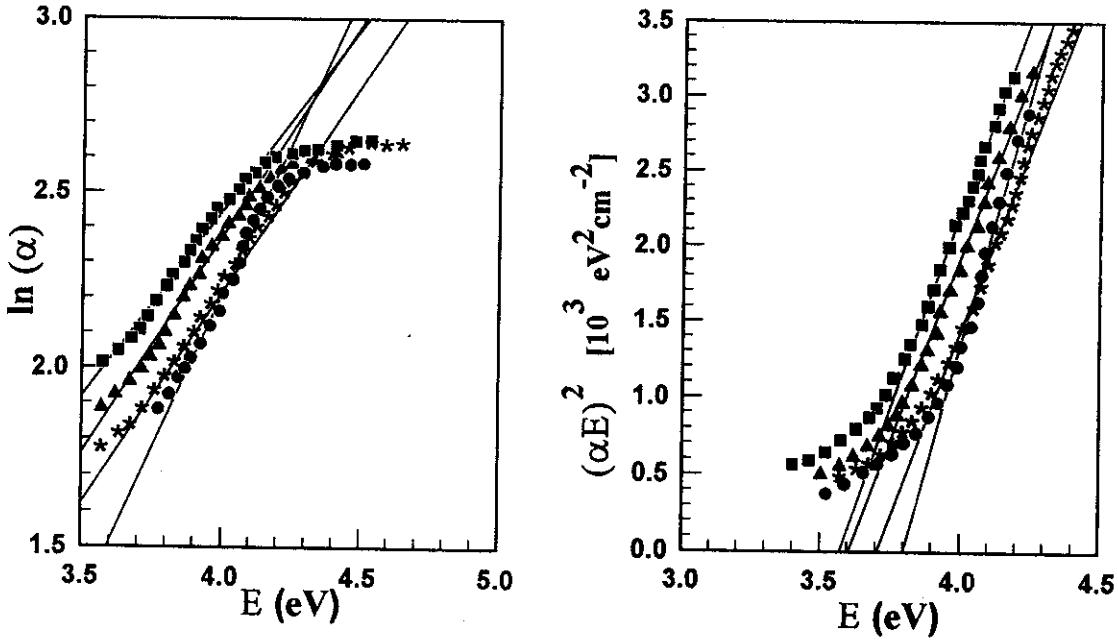

Fig.(IV.19) The dependence of ln (α) and $(\alpha E)^2$ on photon energy (E) for Thermally polymerized PMMA /Perylene sample (•) before and after exposure to unfiltered light (⋆) 20 , (▲) 40 and (▪) 180 minutes.

Table(IV.11): The optical parameters (E_g and E_u) for pure PMMA and PMMA/perylene exposed to unfiltered light .

Preparation	Exposure time (min)	E_g (eV)	E_u (eV)
Pure PMMA			
Thermal	0	4.05	0.26
	20	3.96	0.27
	40	3.69	0.29
	180	3.50	0.30
Casting	0	4.22	0.40
	20	3.90	0.49
	40	3.67	0.53
	60	3.51	0.62
PMMA/perylene			
Thermal	0	3.80	0.63
	20	3.71	0.83
	40	3.61	0.82
	180	3.57	0.93
Casting	0	4.20	0.54
	20	4.15	0.60
	40	4.08	0.67
	60	4.22	0.42

transition (i.e., for n=1/2) [162,163]. The optical gap was determined from the intercept on the energy axis of the linear fit of the large energy data in the plot (Tauc extrapolation)[164,165].

All the corresponding plots shown in Figs.(IV.18,19) illustrate the dependence of E_g on the sample preparation. It is observed that E_g for solvent cast PMMA is larger than that for thermally polymerized one. This can be explained by the following two effects: firstly, in solvent cast PMMA there is a wide distribution of different types of bond energies (see FT-IR results) due to the presence of solvent molecules, this effect causes the increase of E_g. Secondly, in thermally polymerized PMMA there is a poor heat exchange in the system during the polymerization process. Since the polymerization is highly exothermic process, this leads to considerable overheating of the product, and the net result is a polymer of non-uniform mass distribution [109]. Thus the increased degree of disorder lowers the value of E_g[166]. It is noticed that the dependence of E_g on sample preparation does not match with E_u values because the sample having a narrower band gap expected to have a wider band tail. The change in E_u is probably affected by potential fluctuations associated with the polymer structure. Unlike E_u behaviour, E_g is not as greatly affected by inner potential fluctuations because the initial and final states are at practically the same potential [167].

The dependence of $\ln\alpha$ on photon energy E for perylene doped PMMA samples is shown in Figs. (IV.18,19). The corresponding values of E_u is obtained using equation (IV-12) and listed in Table (IV.11). A dramatic increase in E_u is observed by doping PMMA with perylene. This is due to the effect of internal potential fluctuations associated with structural disorder.

The dependence of $(\alpha E)^2$ on photon energy E for doped PMMA samples is shown in Figs. (IV.18,19) and the values of E_g were estimated. They are of the order of other reported values for some polymeric materials and glasses [168,169]. It is found that the value of the band gap energy decreases by doping for thermally polymerized samples while it is not changed for solvent cast samples. This means that the degree of disorder increases in thermally polymerized sample because the dye molecules are caged between the polymer chains. On the other hand the confined solvent molecules in the solvent cast sample introduce localized levels which form a continuum, acting as trapping states.

(IV.D.2) Stability and Degradation

(i) Indoor Testing

PMMA and PMMA/perylene samples were irradiated by direct and filtered artificial sun radiation from Xenon arc lamp. The radiation was filtered from UV component by inserting a water container in the radiation path. Fig.(IV.17) illustrates the change in the absorption spectra of PMMA/perylene samples upon the exposure to unfiltered light. It is observed that the main shoulder characterizing PMMA becomes broader and the peak of perylene is shifted to longer wavelength (red shifted). The broadening of the absorption spectrum of PMMA is attributed to the existence of more transitions from higher vibrational levels of the ground state to higher sublevels of the first excited singlet State. For the thermally polymerized sample the optical density of perylene decreased by 1% after 3 hours exposure but for solvent cast sample the absorption curve became similar to that of pure one after one hour. Also the band tails and band gap energies are estimated after different exposure times to unfiltered Xenon arc light as illustrated in Figs. (IV.18,19). The

obtained values of E_u and E_g are listed in Table (IV.11) which show that E_u increases while the E_g decreases by increasing the exposure time. After 3 hours under these exposure conditions, photodegradation effects induced by unfiltered light (presence of UV component) played a dominant role on the stability of the dye. But for filtered light (absence of UV component), the absorption spectrum does not change, this is confirmed by the optical parameters summarized in Table (IV.12).

Figs. (IV.20,21) show the effect of shelf aging in the dark of pure and perylene doped PMMA samples exposed to unfiltered light for three hours. The optical properties summarized in Table (IV.13), show the complete recovery in the optical properties (where both E_g and E_u increased up to their initial value before exposure). On the other hand for thermally polymerized PMMA /perylene sample the values of E_g and E_u are still lower than their initial values, due to the increase of the degree of disorder associated by dye decomposition.

(ii) Outdoor testing

More long term measurements had to be made to study the photostability of as prepared PMMA/perylene samples under outdoor exposure to sun light for 8 months and the change in the absorption band were studied. The red shift of the absorption peak after exposure to solar radiation is attributed to the excitation processes produced by a photon energy. This results in a change in the chain length (L) and the number of π electrons N[46]. This change is responsible for the appearance of an additional absorption band in the spectral region of emission. In addition, the optical density concerning perylene decreased by 44% after 32 weeks exposure for thermally polymerized sample and 90% after 2 weeks for solvent cast one. This reduction can be attributed to photochemical

Table(IV.12): The optical parameters (E_g and E_u) for pure PMMA and PMMA/perylene samples exposed to filtered light.

Preparation	Exposure time (min.)	E_g (eV)	E_u (eV)
Pure PMMA			
Thermal	0	4.05	0.26
	180	4.03	0.26
Casting	0	4.22	0.40
	180	4.22	0.38
PMMA/perylene			
Thermal	0	3.80	0.63
	180	3.79	0.65
Casting	0	4.20	0.54
	180	4.20	0.53

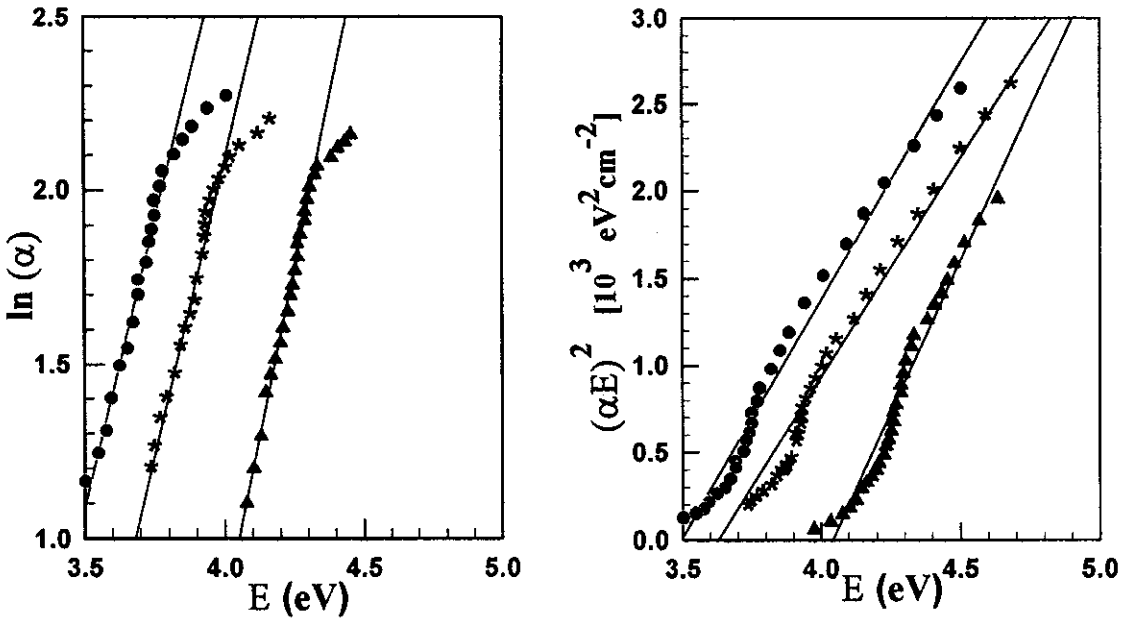

Fig.(IV.20) The dependence of ln (α) and $(\alpha E)^2$ on photon energy (E) for thermally polymerized PMMA sample (•) before and after shelf aging in dark (⋆)1 and (▲) 4 weeks.

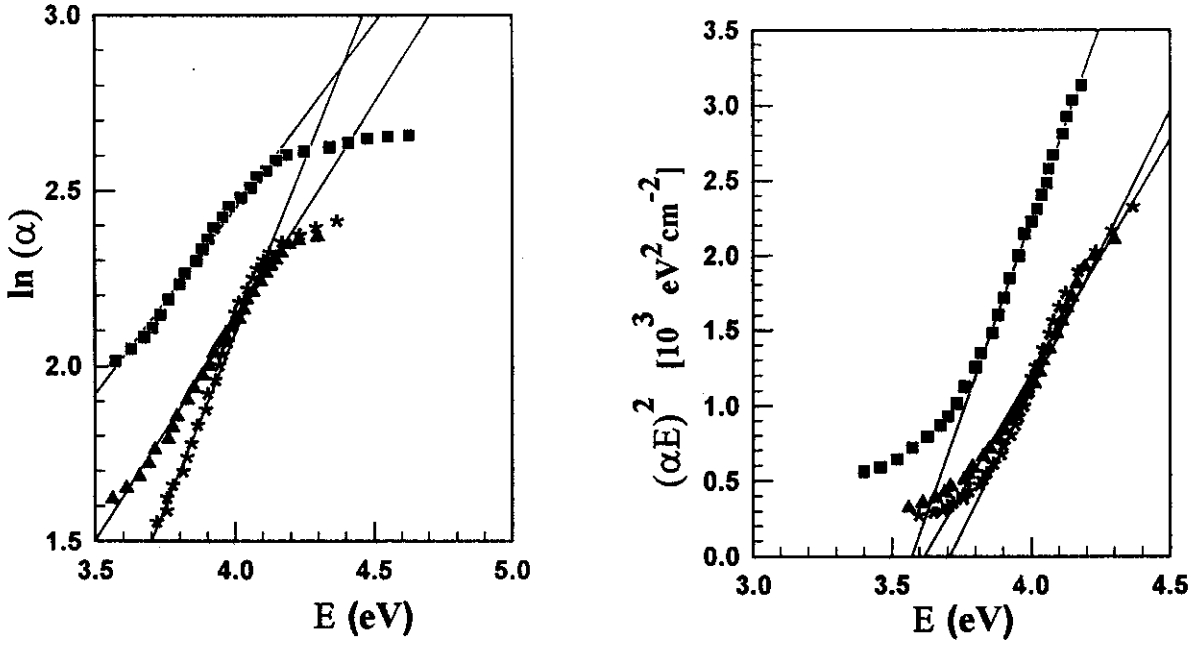

Fig.(IV.21) The dependence of ln (α) and $(\alpha E)^2$ on photon energy (E) for thermally polymerized PMMA/perylene sample, (■) before and after shelf aging in dark (▲)4 and (⋆)8 weeks.

Table(IV.13): The optical parameters (E_g and E_u) after shelf aging of pure PMMA and PMMA/perylene samples exposed to unfiltered light .

Preparation	Aging Time (week)	E_g (eV)	E_u (eV)
Pure PMMA			
Thermal	0	3.50	0.30
	1	3.63	0.29
	4	4.04	0.28
Casting	0	3.51	0.62
	1	3.95	0.47
	4	4.22	0.42
PMMA/perylene			
Thermal	0	3.57	0.93
	4	3.62	0.81
	8	3.71	0.52
Casting	0	4.22	0.42
	4	4.22	0.39
	8	4.20	0.41

decomposition of the dye caused by the absorption of UV part of the solar spectrum, since the absorbed quantum is higher than the energy of any bond molecule. The solar bleaching of solvent cast PMMA/perylene sample after exposure to sunlight for 8 months ,is shown in Fig.(IV.22)

Photodegradation of perylene (P%) , the percentage change of the absorption peak, has been estimated after exposure of a thermally polymerized sample of concentration ($6.33x10^{-5}$ mol.%) for 32 weeks and is given in Fig.(IV.23) . The plot of P% versus the exposure time t suggests two regions of degradation obeying the relation,

$$P = P_o e^{-Rt} \qquad \textbf{(IV-14)}$$

where $P = P_o$ at $t = 0$ and R is the photodegradation rate of perylene dye. This exponential decay fitting is in good agreement with other literatures[50,81]. The obtained decomposition rates for the two regions (from the short to longer exposure time) are 6×10^{-8} and 2.2×10^{-8} $sec.^{-1}$ respectively. This clearly illustrates that the decomposition rate is decreased to one third of its value after 70 days of exposure .

Table (IV.14) shows that the values of E_g and E_u for pure PMMA samples do not change after exposure to sun light for 8 months. This means that the change occurred in the samples during the day exposure vanished by the dark reactions which occur under the day night cycles. On the other hand for PMMA/ perlyne sample prepared by casting method the optical gap has the same value of that of the pure one after exposure to sunlight. This is due to the complete bleaching of dye after two weeks of outdoor exposure. From these observations thermal polymerization of PMMA is preferable in outdoor applications, because

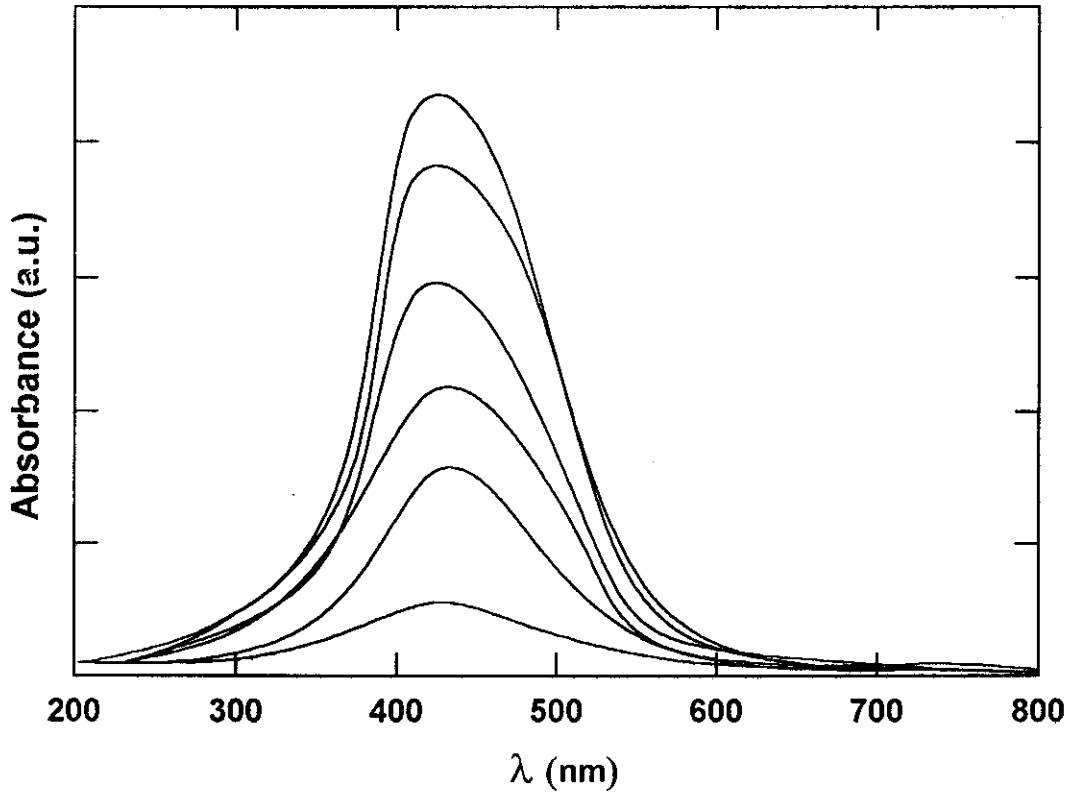

Fig.(IV.22) The solar bleaching of solvent cast PMMA/perylene sample exposed to day light for 8 months.

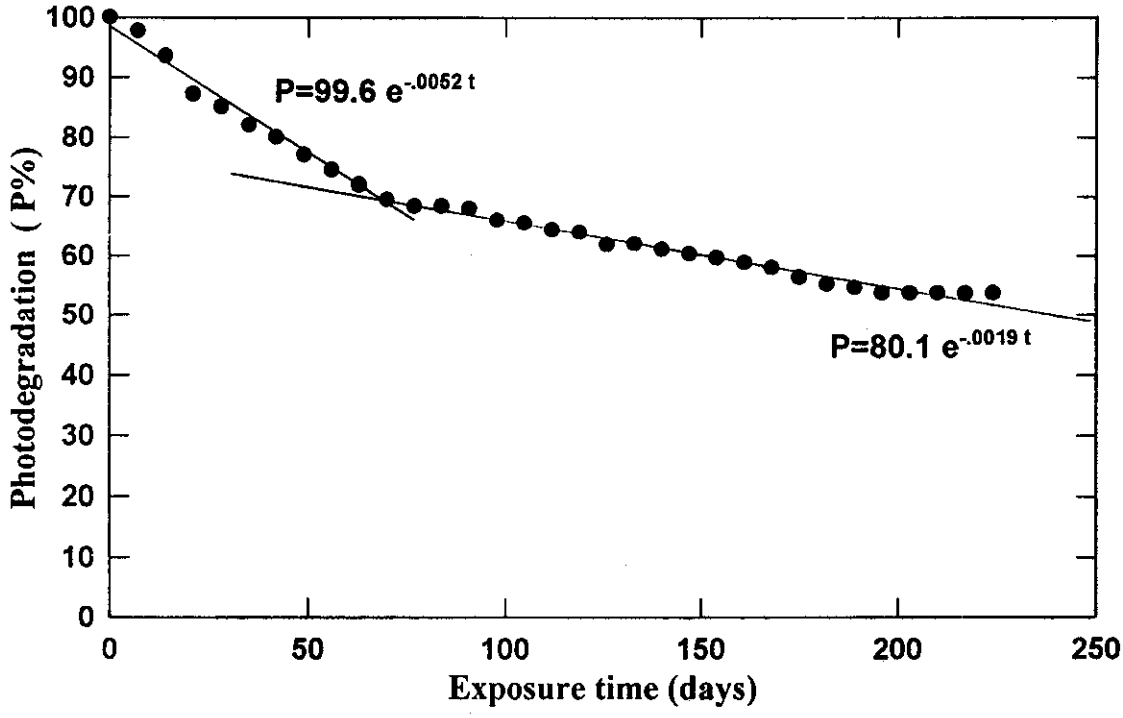

Fig.(IV.23) The photodegradation curve of thermally polymerized PMMA/Perylene sample after outdoor exposure to day light for 8 months.

Table (IV.14): The optical parameters (E_g and E_u) for pure and perylene doped PMMA exposed to sun light .

Preparation	Exposure time (week)	E_g (eV)	E_u (eV)
Pure PMMA			
Thermal	0	4.05	0.26
	1	4.02	0.40
	10	3.94	0.50
	32	3.98	0.51
Casting	0	4.22	0.40
	1	4.18	0.31
	10	4.15	0.33
	32	4.19	0.29
PMMA/perylene			
Thermal	0	3.80	0.63
	1	3.77	0.57
	10	3.63	0.62
	32	3.57	0.66
Casting	0	4.20	0.54
	1	3.95	0.65
	10	3.97	0.53
	32	4.20	0.48

of the reducing the strong UV degradation of the dye for FSCs.

To estimate a fundamental rule involved in the outdoor degradation of the samples, the dependence of ln α and $(\alpha E)^2$ on photon energy E was tested in the range from room temperature to 403 K. The corresponding energy band gap E_g and Urbach's energy E_u were calculated and listed in Table (IV.15). It is observed that there is no major thermal effect on E_g and E_u below T_g of the samples , this is in agreement with published data[50].This means that the photo-degradation process of polymer and dye depends only on the incident photon energy (E).This is expected because the photodegradation measurements which were made indoor and outdoor performed at ambient temperatures not up to 50 °C which is much lower than T_g values of the samples.

(IV.D.3) Fluorescence Measurements

The fluorescence characteristics of PMMA/perylene have been measured to detect the photodegradation of perylene dye and the overlap of their absorption and emission spectra, which strongly affect the FSC performance. The emission spectra of thermally polymerized PMMA /perylene show a dependence on perylene dye concentration as shown in Fig. (IV.24). It is noticed that the sample of concentration ($6.33x10^{-5}$ mol.%), has the highest fluorescence intensity and the most red-shifted spectrum.

The Stokes shift, defined as the difference between the absorption and emission maxima was evaluated for different perylene concentrations and listed in Table (IV.16). It is observed that the Stokes shift decrease by increasing dye concentration, this indicates a larger self-absorption of the emitted radiation by the dye molecules.

Table (IV.15): The optical parameters (E_g and E_u) for pure and perylene doped PMMA at different temperatures.

Preparation	Temperatue (K)	E_g (eV)	E_u (eV)
Pure PMMA			
Thermal	300	4.05	0.26
	343	4.06	0.26
	363	4.05	0.27
	393	3.90	0.35
Casting	300	4.22	0.40
	323	4.2	0.43
	343	4.09	0.54
PMMA/perylene			
Thermal	300	3.80	0.63
	343	3.81	0.63
	363	3.83	0.68
	393	3.69	0.79
Casting	300	4.20	0.54
	323	4.19	0.52
	343	4.06	0.69

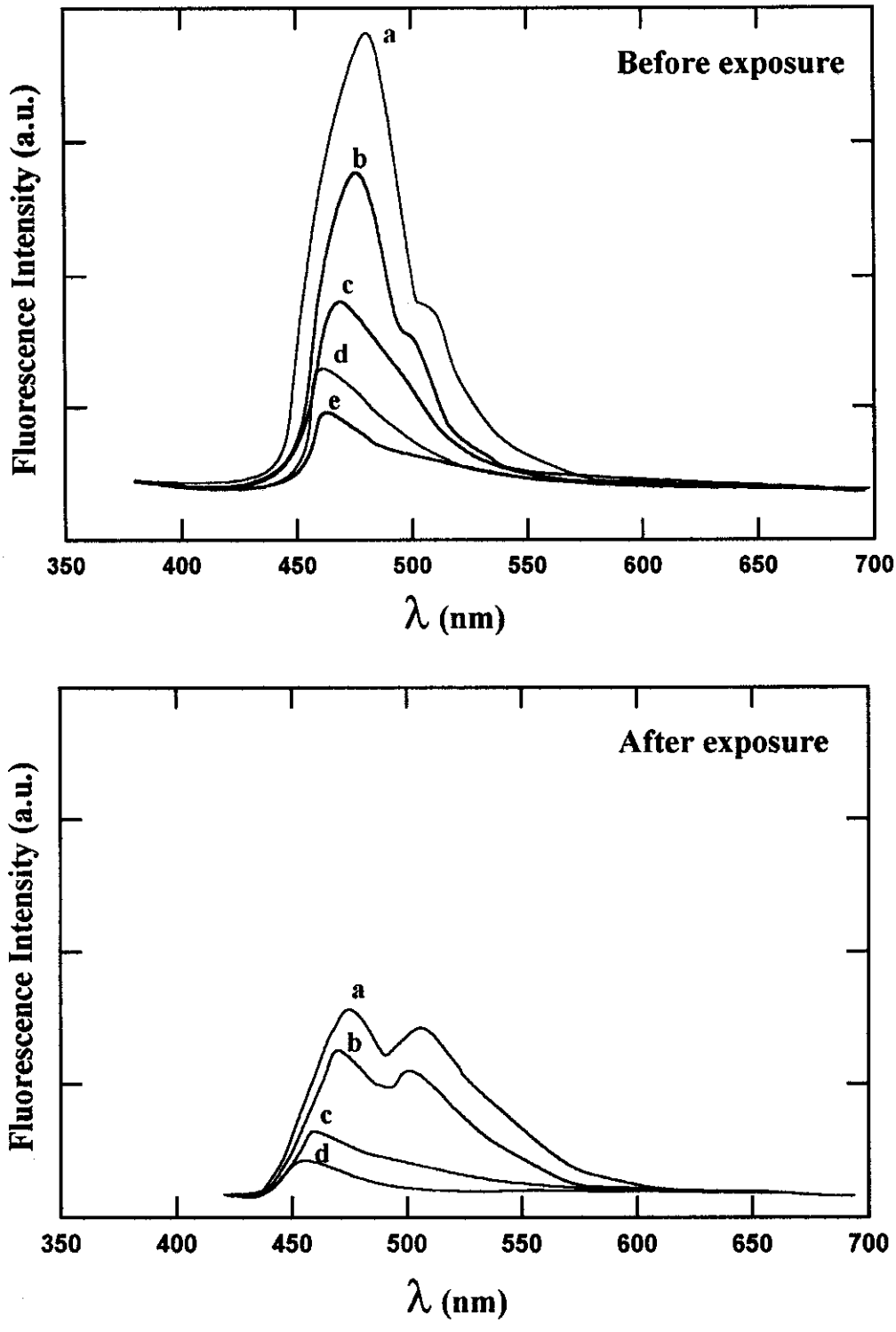

Fig.(IV.24) **Fluorescence spectra of thermally polymerized PMMA / Perylene samples before and after outdoor exposure to sun light for Summer (2000), (a) 6.33 x 10^{-5}, (b) 7.92 x 10^{-5}, (c) 1.06 x 10^{-4}, (d) 1.38 x 10^{-4} and (e) 2.11 x 10^{-4} mol.% .**

Table(IV.16): The effect of concentration on the spectroscopic properties of Perylene dye doped in PMMA before and after exposure to sunlight.

(a) Before exposure.

Concentration mol.%	λ_{abs} (nm)	λ_{em} (nm)	$\Delta\lambda_s$ (nm)	ϕ_f %
6.33×10^{-5}	405.9	479.2	73.3	94.8
7.92×10^{-5}	401.6	473.3	71.7	87.2
1.06×10^{-4}	400.0	467.9	67.9	76.9
1.38×10^{-4}	396.8	462.2	65.4	65.8
2.11×10^{-4}	390.3	459.8	62.7	58.3

(b) After exposure.

Concentration mol.%	λ_{abs}(nm)	λ_{em} (nm)	$\Delta\lambda_s$ (nm)	ϕ_f %
6.33×10^{-5}	412.8	475.0	62.2	79.8
7.92×10^{-5}	412.8	471.25	58.5	71.2
1.06×10^{-4}	411.0	461.2	50.2	60.3
1.38×10^{-4}	408.2	453.8	45.6	56.8

The fluorescence quantum yield ϕ_f has been measured relative to BASF-241 doped in PMMA as a reference (ϕ_f ~99%)[170], and calculated from the following equation [124],

$$\phi_f = \phi_{f,ref} (A_{ref}/A) (n/n_{ref}) (a/a_{ref}) \qquad \text{(IV-15)}$$

where $\phi_{f,ref}$ is the fluorescence quantum yield of a reference, A is the absorbance, n the index of refraction and a is the area under fluorescence curve, the obtained values of ϕ_f for different perylene concentrations are listed in Table (IV.16). It is observed that the highest ϕ_f and largest Stokes shift obtained for perylene concentrations 6.33×10^{-5}, 7.92×10^{-5} and 1.06×10^{-4} mol.%. Therefore, these concentrations have been selected for field performance of fluorescent solar collectors (FSCs).

After the samples exposed to daylight illumination for one season (Summer 2000), it is found that a new fluorescence band appears as shown in Fig. (IV.24), and the fluorescence quantum yield decreases as observed in Table (IV.16). The appearance of this new band is due to the formation of dimers that exist only in the excited state (excimers), and are generally weakly fluorescent [122].

(IV.D.4) Field Performance of FSCs

(i) Time Variation of Global Solar Radiation

The daily global solar radiation falling on a horizontal surface was measured hourly for one season (Summer 2000), using an accurate silicon sensor irradiance byranometer. As shown in Fig. (IV.25), it is noticed that the curve of global solar radiation versus the time of the day reaches its maximum at the noon.

Fig. (IV.26) illustrates the hourly proportions of the direct and diffused radiation falling on a horizontal surface during Summer 2000. It is noticed that most of the global radiation near the sunrise and sunset is diffused, to which the photovoltaic cells are not efficient. This problem will be solved by using FSCs, as will be shown in the following sections.

Figs.(IV.25,26) can also give us valuable information about, the sunrise time, the sunset time, the peak power at solar noon and determining of the day length. These curves are also useful when designing a photovoltaic system to satisfy the electrical energy demand.

(ii) Effect of Orientation and Output Power Correlations

In Photovoltaic (PV) applications of FSCs the effect of tilt angle is very important. Tilting a surface up from the horizontal position decreases the diffused radiation and subsequently increases the reflection received from the ground. For photovoltaic array applications the tilt angle is often ranged between Lat.+20 to Lat.–20[171], where Lat. is the angle that specify the collector location on earth with respect to sun " latitude angle"[10]. But in our study the FSC tilt angle is ranged between Lat. +10 to Lat-10. In PV array applications, tracking technique may

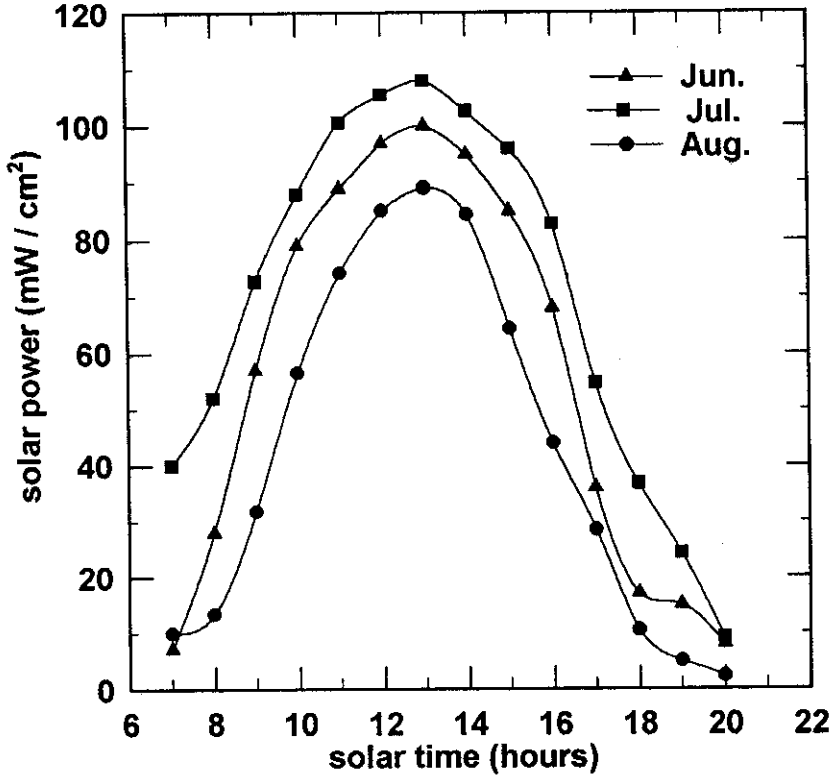

Fig.(IV.25) The hourly distribution of global solar radiation for Summer (2000).

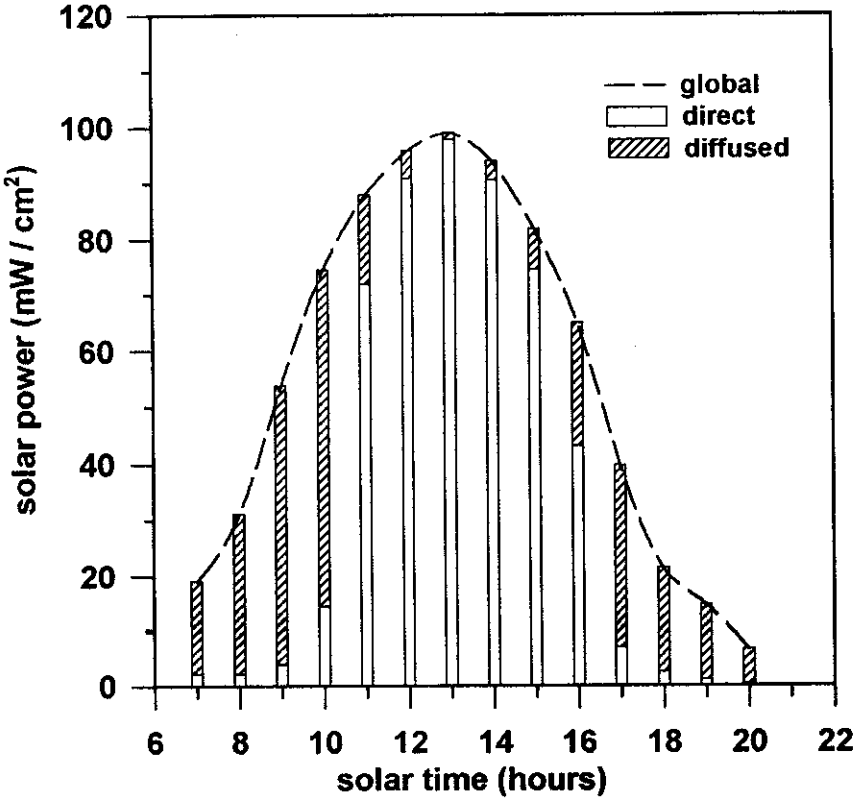

Fig.(IV.26) The mean hourly global solar radiation for Summer (2000) and the proportions of direct and diffused components.

duplicate the amount of solar radiation falling on the array [172,173] in contrast to our results which will show that the effect of tilt and tracking are not necessary.

For practical performance expectation, a correlation between output power of the horizontal position and both optimum tilt and tracking positions had to be made. Fig. (IV.27) shows the non-linear correlations for the output power of the FSCs at a horizontal P_h and both optimum tilt P_o and tracking P_t. The correlation equations obtained for Summer season are:

$$P_o = \alpha_o P^2_h + \beta_o P_h + \gamma_o \qquad \text{(IV-16)}$$

$$P_t = \alpha_t P^2_h + \beta_t P_h + \gamma_t \qquad \text{(IV-17)}$$

The fitting parameters α,β,γ for optimum and tracking positions are obtained and listed in Table (IV.17). It can be seen that the dependence on sun tracking increases by increasing the perylene concentration. Furthermore the effect of tilt and tracking did not give a significant increase in the output power of the horizontal position. These results are in agreement with published data [81], and will be explained by the following study.

(ii) Optical Efficiency

The optical efficiency $\eta_{opt.}$, of the plates is calculated using the equation[25],

$$\eta_{opt} = \frac{P_{out}}{P_{in}} = \frac{I_{sc}}{I_{ref}} \times \frac{R_\lambda}{R_{sun}} \times \frac{1}{G} \qquad \text{(IV-18)}$$

where I_{sc} and $I_{ref.}$ are the output current of the solar cell attached to the

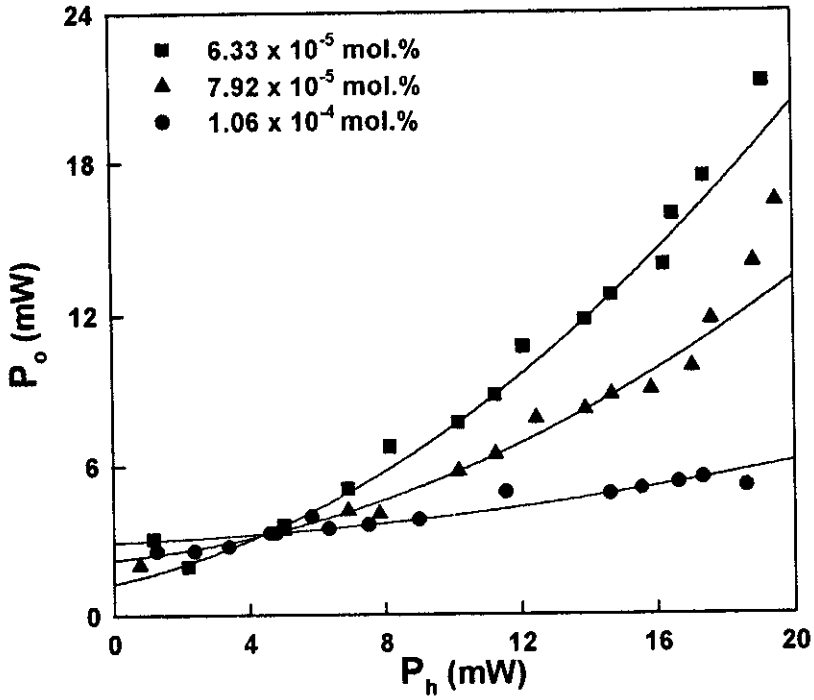

Fig.(IV.27.a) Effect of dye concentration on the hourly output power correlations between the horizontal P_h and optimum tilt P_O positions for FSCs during Suummer (2000).

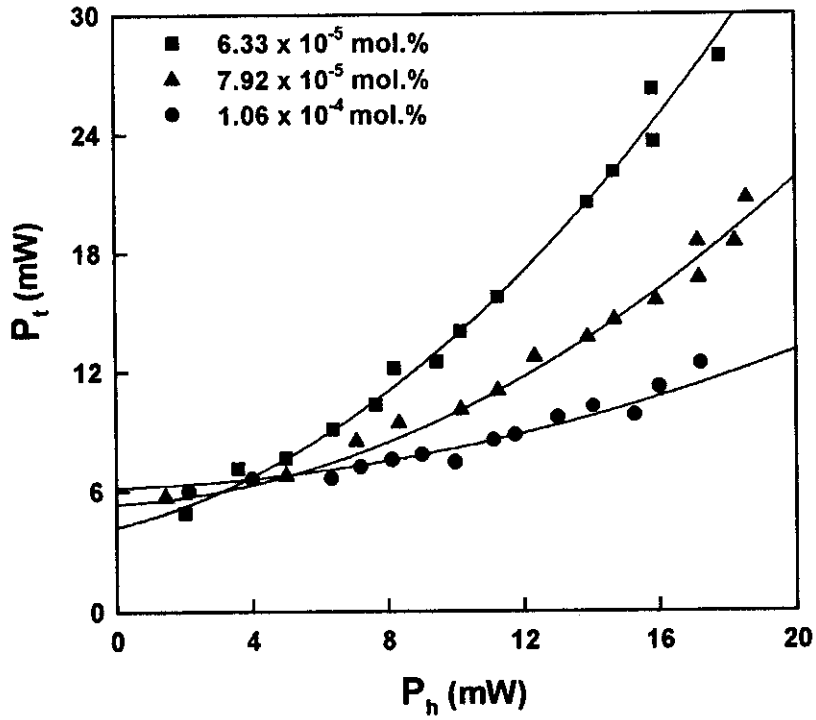

Fig.(IV.27.b) Effect of dye concentration on the hourly output power correlations between the horizontal P_h and tracking P_t positions for FSCs during Suummer (2000).

Table(IV.17): The obtained coefficients in output power correlations for FSCs in Summer 2000

Concentration mol. %	α_o	α_t	β_o	β_t	γ_o	γ_t
$6.33x10^{-5}$	0.009	0.786	0.010	1.100	0.232	0.057
$7.92x10^{-5}$	0.012	0.842	0.022	0.940	0.510	0.702
$1.06x10^{-4}$	0.018	0.813	0.027	1.040	0.279	0.469

edge of the collector and the reference solar cell respectively, G is the geometric gain , (defined as the ratio of the top surface area to the edge area of the collector). R_λ and R_{sun} are the response of the solar cell at emitted wavelength and the solar spectrum respectively. Three different positions were considered; horizontal, optimum tilt and tracking. The results of operating the FSCs were obtained during the day light (from 7 A.M. to 8 P.M.) in Summer 2000 and are shown in Fig.(IV.28). It is noted that the optical efficiency increases near both the sunrise and sunset and becomes shallower around the midday. From the practical point of view this behaviour is advantageous, since the better utilization of the FSC is achieved when both direct solar radiation and sensitivity of the solar cell decreases as shown in Figs.(IV.26&29) respectively. Furthermore Summer average values of hourly optical efficiency obtained are higher than the previous work [50,81,82]. This is attributed to the higher sensitivity of the used solar cell and coincidence of its spectral response with the emitted wavelength from FSCs as illustrated in Fig.(IV.30). Table (IV.18) shows that the plate of PMMA having perylene concentration 6.33×10^{-5} mol.%, have the highest values for the optical efficiency due to low self-absorption (large Stokes shift) and large fluorescence quantum yield (ϕ_f)[174,175]. Moreover the obtained values of the optical efficiency presented in Table (IV.18) at three positions recommend the horizontal mounting of FSCs because the cost of energy required to track the sun outweighs the extra energy obtained by the collector.

(iv) Effect of ambient temperature and partial shading

Fig.(IV.31) shows the effect of ambient air temperature on the performance of FSCs. It is noticed that the plate temperature going with

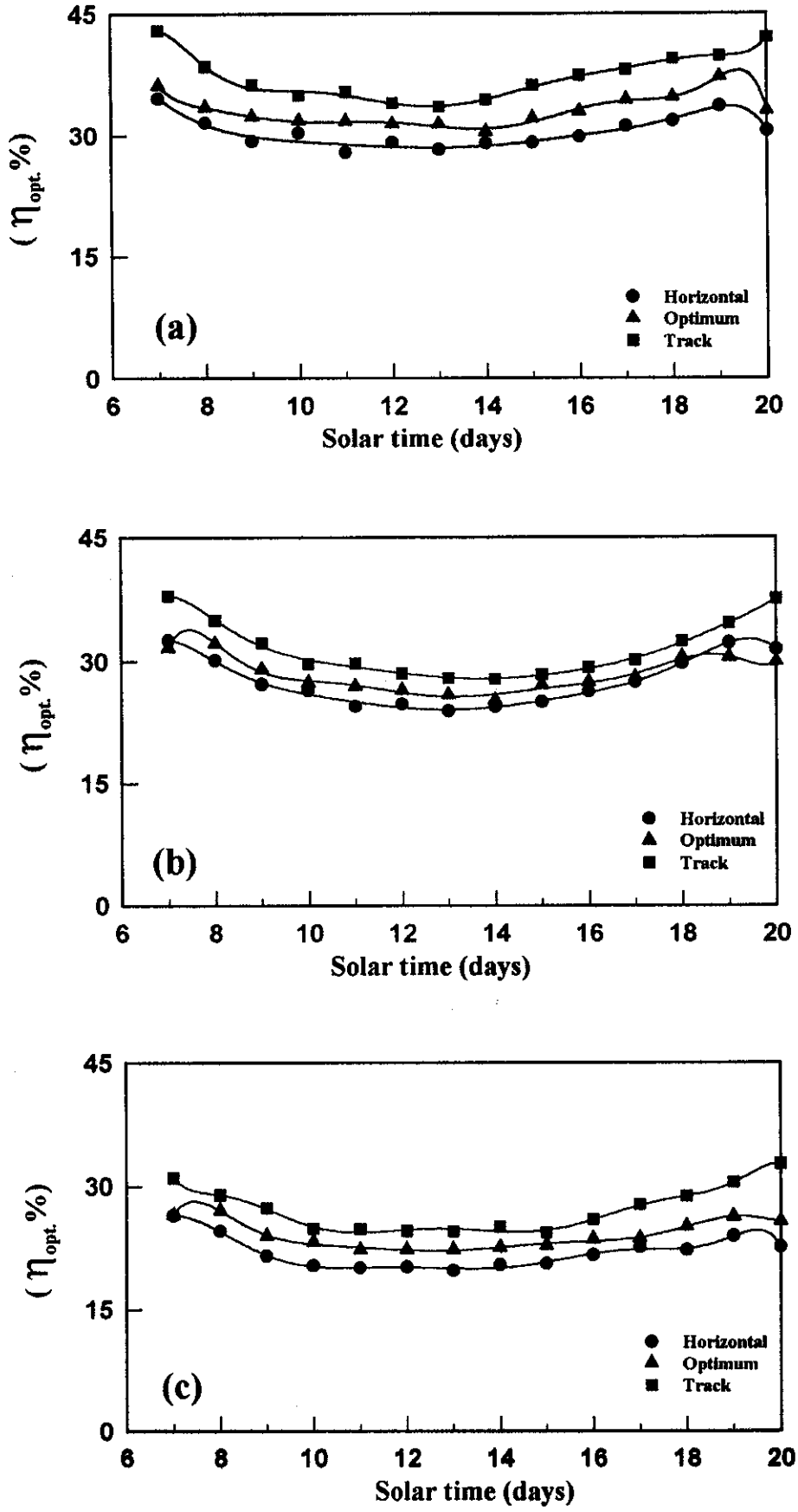

Fig.(IV.28) The hourly optical efficiency of PMMA/Perylene solar collectors of concentrations (a)6.33 x 10^{-5},(b) 7.92 x 10^{-5},(c)1.06 x 10^{-4} mol.% tested at different positions during one season (Summer 2000).

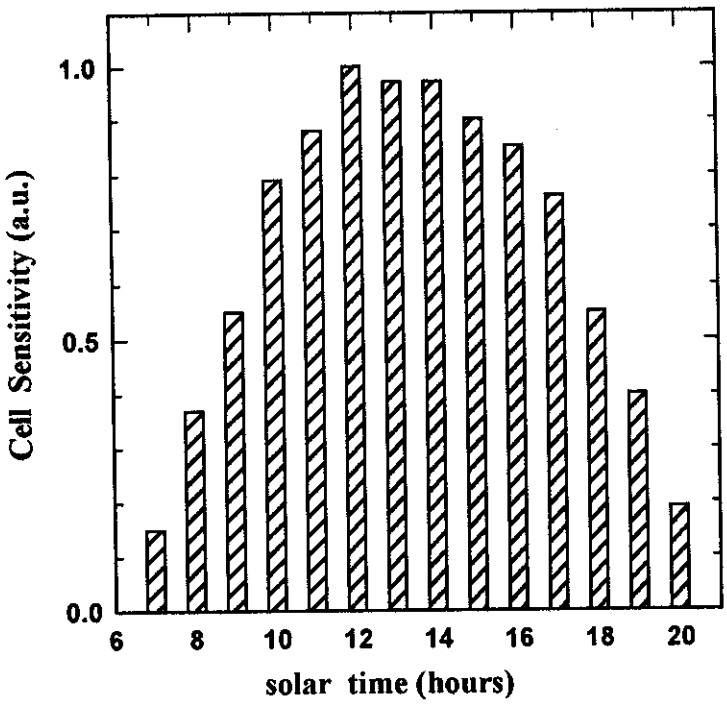

Fig.(IV.29) The hourly sensitivity of the solar cell during the day.

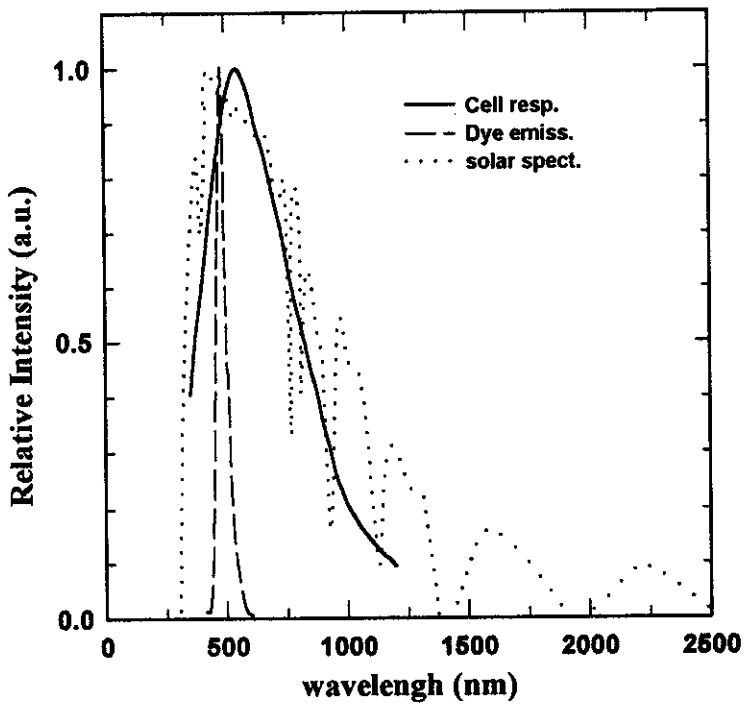

Fig.(IV.30) The spectral response of the solar cell , the solar spectrrum at different air masses and the emission spectrum of the collector (6.33×10^{-5}mol.%).

Table (IV.18): Summer average values of hourly optical efficiency (η_{opt}%) for PMMA / Perylene FSC$_s$.

Concentration mol. %	η_{opt} %		
	Horizontal	Optimum	Track
6.33×10^{-5}	30.4	33.1	37.3
7.92×10^{-5}	27.5	28.4	31.5
1.06×10^{-4}	21.9	24.1	27.2

the same trend as the ambient air temperature. On the other hand, Fig. (IV.28) shows that the optical efficiency increases around the sunrise and sunset (low ambient air temperatures), this phenomenon may be due to the thermal effect on photon trapping inside the plate and the fluorescence quantum yield[120-122].

The effect of partial shading which causes a severe decrease in the output power and efficiency of the solar cell has been studied , both the FSC of perylene concentration 6.33 $x10^{-5}$ mol.% and the reference solar cell was shaded at noon using diffusing glass plates with different thicknesses. Fig. (IV.32) shows that the output efficiency of the reference cell decreases to almost zero, while the FSC still keeps about 83% of its efficiency. Because the collector cell is collecting light from wide area of the fluorescent plate it is less sensitive to partial shading. This reflects an excellent advantage of the FSC[1,56].

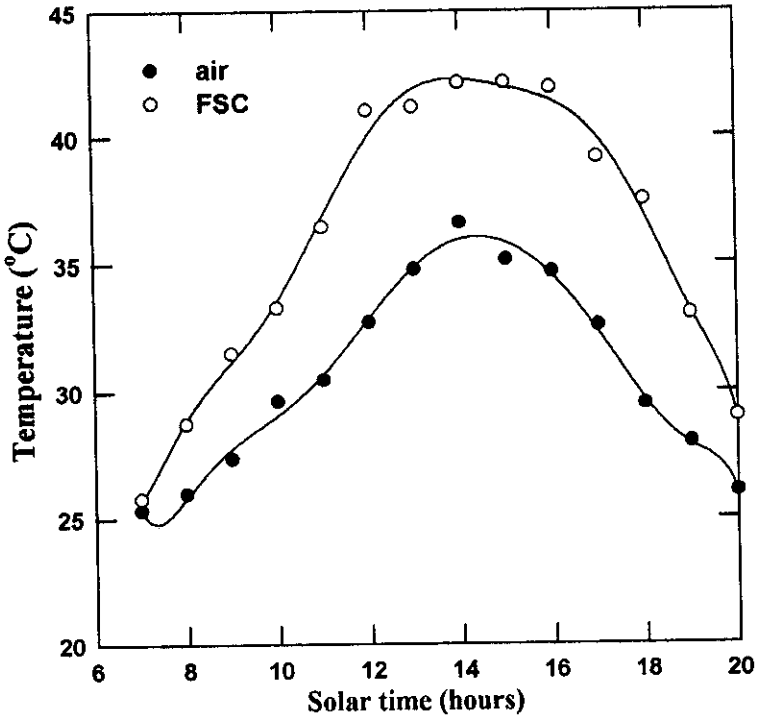

Fig.(IV.31) The hourly variation of ambient air and FSC temperatures during Summer 2000.

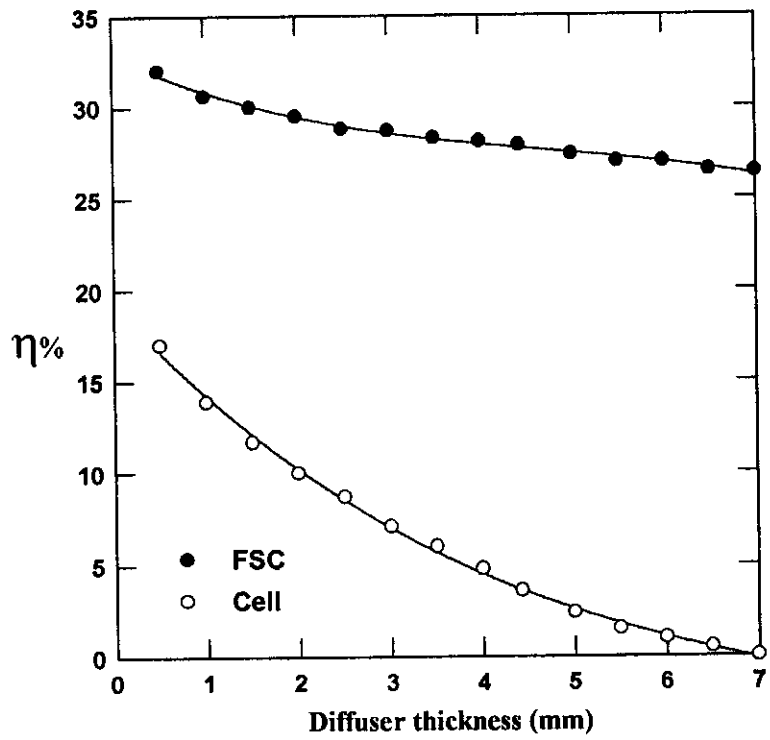

Fig.(IV.32) The effect of partial shading on the efficiency of both the solar cell and FSC tested at noon (100 mW/cm^2).